The role of local atmospheric forcing on the modulation of the ocean mixed layer depth in reanalysis and a coupled single column ocean model

Article

Accepted Version

The role of local atmospheric forcing on the modulation of the ocean mixed layer depth in reanalyses and a coupled single column ocean model

Byju Pookkandy [1]*, Dietmar Dommenget [1], Nicholas Klingaman [2], Scott Wales [3], Christine Chung [4], Claudia Frauen [5], Holger Wolff [1]

[1] ARC Centre of Excellence for Climate System Science, School of Earth Atmosphere and Environment, Monash University, Clayton, Victoria, Australia

[2] National Centre for Atmospheric Science-Climate and Department of Meteorology, University of Reading, UK

[3] ARC Centre of Excellence for Climate System Science, School of Earth Sciences, The University of Melbourne, Australia

[4] Bureau of Meteorology, Melbourne, Australia

[5] CNRM-GAME (Météo-France/CNRS), Toulouse, France

* Corresponding author:

Byju Pookkandy

byju.pookkandy@monash.edu

Ph: +61-3-990-54495

Abstract

The role of local atmospheric forcing on the ocean mixed layer depth (MLD) over the global oceans is studied using ocean reanalysis data products and a single-column ocean model coupled to an atmospheric general circulation model. The focus of this study is on how the annual mean and the seasonal cycle of the MLD relate to various forcing characteristics in different parts of the world's oceans, and how anomalous variations in the monthly mean MLD relate to anomalous atmospheric forcings. By analysing both ocean reanalysis data and the single-column ocean model, regions with different dominant forcings and different mean and variability characteristics of the MLD can be identified. Many of the global oceans' MLD characteristics appear to be directly linked to the different atmospheric forcing characteristics at different locations. Here, heating and wind-stress are identified as the main drivers; in some, mostly coastal, regions the atmospheric salinity forcing also contributes. The annual mean MLD is more closely related to the annual mean wind-stress and the MLD seasonality is more closely related to the seasonality in heating. The single-column ocean model, however, also points out that the MLD characteristics over most global ocean regions, and in particular in the tropics and subtropics, cannot be maintained by local atmospheric forcings only, but are also a result of ocean dynamics that are not simulated in a single-column ocean model. Thus, lateral ocean dynamics are essential in correctly simulating observed MLD.

Key words: Ocean mixed layer depth; Atmospheric forcings; Coupled single column ocean model; Annual mean; Seasonal variability; Flux correction

1. Introduction

The processes occurring in the upper ocean are predominantly forced by the atmosphere. Heating and cooling at daily to seasonal scales, wind-stress, evaporation and precipitation are the dominant physical processes that act on and interact with the upper layer of the ocean. Vigorous turbulent mixing near the surface by these forces results in a layer of homogeneous temperature and salinity (and thus density); its depth is defined as the ocean mixed layer depth (MLD).

Understanding the physics of the MLD is important for climate dynamics, because the thickness of the mixed layer (ML) modulates its heat capacity and hence its ability to store excess heat from the atmosphere (Godfrey and Lindstrom 1989; Maykut and McPhee 1995; Swenson and Hansen 1999; Peter et al. 2006; Dong et al. 2007; Montégut et al. 2007). In addition, MLD variations over the seasonal cycle or anomalies from it are one of the main processes for exchanging heat between the atmosphere and the deeper oceans. Proper quantification of the ML heat budget is important as it governs the evolution of the sea surface temperature (SST) (Chen et al. 1994; Alexander et al. 2000; Dommenget and Latif 2002; Qui et al. 2004; Dong et al. 2008). In a study using a simple stochastic model, Dommenget and Latif (2008) showed that the low frequency (e.g., decadal) variability in SST is a result of the interaction of the heat stored in the layers below the MLD and the heat in the mixed layer. It thus suggests that decadal SST variability strongly depends on how the MLD varies and interacts with the subsurface layers. According to them the sensitivity of SST to MLD variability maximizes in the midlatitudes. Therefore, seasonal to interannual, and maybe even decadal, variability in SST can be simulated in terms of the local air-sea interactions and proper representation of MLD variability. Mixed-layer dynamics are also important for the ocean's biological productivity (Fasham 1995; Polovina et al. 1995; Narvekar and Kumar 2006) and acts as a medium for exchange of trace gases between the ocean and the atmosphere (Takahashi et al. 1997; Bates 2001; Sabine et al. 2004).

A number of studies have examined the mixed layer dynamics and demonstrated the variation in MLD at different spatial and temporal scales (Montery and Levitus 1997; Kara et al. 2000; Cronin and Kessler 2002; Kara et al. 2003; Montégut et al. 2004; Halkides and Lee 2009). Most of these studies were limited to either a small region or at specific locations where in-situ data is available, and then extrapolated over a wider domain using some specific techniques. Since the advent of Argo data, reanalysis methods have produced a much more reliable source of representations of the state of the ocean at global scale. It has been shown that in summer the MLD is dominated by entrainment due to wind-induced mixing, whereas

in winter surface buoyancy forcing is the main driver (Alexander et al. 2000). These theories represent generalised concepts of MLD variability in the global ocean. However, the relative role of these forcings varies in time and space. This uneven distribution of MLD forcing on the seasonal time scale is not understood in detail over the global ocean. Lorbacher et al. (2006) and Carton et al. (2008) examined the variability in MLD at global scale from observations, but these are sparse over the Southern Ocean. Numerous attempts have been made to understand the ocean surface boundary layer and its sensitivity to atmospheric forcing (e.g., Adamec and Elsberry 1984; Large and Crawford 1995; Kantha and Clayson 1994), but again they have mostly been limited to one location or in a small ocean basin.

The focus of the present study is to examine the mean, seasonal cycle and variability of the MLD over the global ocean and how it relates to the different atmospheric forcings and the upper-ocean stratification. The aim is to understand the driving mechanisms of the MLD in different regions and to what extent these can be understood by the local air-sea interactions. In this we will focus on open ocean regions and do not discuss sea ice regions or shallow coastal ocean regions. Therefore, the MLD and the atmospheric forcing terms will be analysed in ocean reanalysis data and in a single-column mixed layer ocean model coupled to an atmospheric general circulation model (AGCM). The latter model simulation allows insight as to what extent the MLD characteristics can be simulated just by local air-sea interactions. It also allows us to diagnose the limitations of local air-sea interactions assumption by analysing the flux correction terms used in the model to maintain a density profile close to the observed mean profile.

The paper is organized as follows: A detailed description of the reanalysis data used, the coupled model and the method to estimate the MLD is presented in the following section. Section 3 focuses on the observed characteristics of MLD estimated from reanalysis data. In section 4 most of the analysis is repeated for the single-column model simulation. Finally, the results are summarised and discussed in section 5.

2. Data, Model and Methods

Reanalyses and data from a single-column ocean model are used to understand the characteristics of the global ocean mixed layer depth and its relation to local atmospheric forcing. Details of the datasets and methods used in this study are described below.

a. Reanalysis data sets

The characteristics of the MLD presented here are partly based on vertical profiles of temperature and salinity from the German contribution to Estimating the Circulation and Climate of the Ocean system (GECCO2) for the period 1948-2011. The data has a spatial resolution of 1x1 degrees in longitude and latitude and comprises 50 vertical levels. The synthesis used model assimilation with available hydrographic and satellite data. A complete description of this data is given by Kohl (2014). Two other data assimilation products are also analysed in addition to GECCO2: The Global Ocean Data Assimilation System (GODAS) data (Behringer and Xue 2004) implemented at National Centers for Environmental Prediction (NCEP) for the period 1980-2013 and the Simple Ocean Data Assimilation (SODA v2.2.4) data for the period 1950-2010 (Carton and Giese 2008). In the following analysis we will focus all analyses on GECCO2, because it provides data for a longer time period than the NCEP-GODAS dataset and compared to the SODA dataset the results appear to be slightly less noisy. The reanalyses are a combination of model dynamics and sparse observational data, therefore one can expect biases between the products that arise from different assimilation procedures (Kröger et al. 2012). Overall the results we present in this study are qualitatively the same in all three datasets. Any significant differences are pointed out in the text.

b. The coupled single column ocean model (ACCESS-KPP)

A 50-year simulation of a coupled atmosphere-ocean single-column model is used to study the MLD variability over the global ocean. The atmospheric component of the coupled model consists of the Australian Community Climate and Earth-System Simulator (ACCESS) version 1.3 atmospheric GCM, which is similar to the UK Met Office's Global Atmosphere version 1.0 with the addition of some modifications included by the Centre for Australian Weather and Climate Research (CAWCR). A horizontal resolution of 3.75º longitude by 2.5º latitude (referred to as N48) and 38 vertical levels are applied in this model setup. A detailed description of the atmospheric model is given in Bi et al. (2013).

The ocean component of the coupled model consists of a single-column first-order nonlocal K-Profile Parameterisation (KPP) mixed layer model, which uses the vertical mixing scheme of Large et al. (1994). It comprises 40 vertical levels with the layer thickness increasing exponentially from the surface to 1000m deep. The single-column ocean model is coupled to the atmospheric model at every ocean grid point of the atmospheric model, and at the time step of both atmosphere and oceanic models (30min), following Klingaman and Woolnough (2014) and Hirons et al. (2015). The KPP model is very adaptable and flexible; it can be

applied to AGCM of any resolution. The atmospheric model provides the surface heat flux, wind-stress and freshwater flux (evaporation minus precipitation or E-P) to the ocean at each time step. The mixed layer model does not represent processes such as horizontal advection or upwelling from below the limited vertical domain. Mixing in the interior (layer bellow the surface) is governed by shear instability, which is modelled as a function of the local gradient Richardson number. A boundary layer depth is determined at each grid point, based on the critical value of the turbulent processes parameterised by a bulk Richardson number. Vertical diffusivity coefficients due to turbulent shear are estimated in the diagnosed boundary layer depth. Mixing is strongly enhanced in the boundary layer in both convective and wind driven situations enabling boundary layer properties to penetrate well into the thermocline. A detailed description of the first order nonlocal KPP fundamentals is given in Large et al. (1994). The ocean model is embedded with varying sea-ice concentration at the higher latitudes. The sea ice variability is simulated by a simple thermodynamical model of melting and freezing of sea ice by local forcings. However, regions with sea ice will not be discussed in this study. A flux correction is applied to the ocean temperature and salinity tendency in order to reduce the climate drift, which is described in the following sub-section.

c. Flux corrections

The ACCESS-KPP model computes the diffusivity profiles at each grid point and then estimates the temperature and salinity profiles. Since ocean dynamics (mainly advection) are absent in the model the temperature and salinity drifts away from the observed reference values for a longer run (many decades). So it is necessary to add flux corrections in order to prevent climate drift. The flux correction values are computed such that the mean seasonal cycle of temperature and salinity closely follow the climatology from WOA09 (Antonov et al. 2010; Locarnini et al. 2010). The temperature and salinity flux corrections are obtained in a number of iterations with the ACCESS-KPP model, where temperature and salinity are free to evolve. In each iteration biases between the model variables and the climatological values are then computed and added as an additional forcing to the model's tendency equation in the next iteration. This process is repeated until the biases between the model variables and the climatological reference values are sufficiently small. The flux corrections vary at each grid point and for each month of year but are state independent and remain the same from one year to the next. Characteristics of the flux correction terms are discussed in the analysis section (see section 4.4).

d. Method for MLD estimation

A wide range of criteria exists for defining MLD from the vertical profiles of temperature, salinity or density. Generally, these criteria fall into two categories: the difference criteria and the gradient criteria. The difference criteria define the MLD as the depth where the oceanic property has changed by a critical value from a reference depth near to the surface (Kara et al. 2000; Montégut et al. 2004). The gradient criteria detect the shallowest depth where the vertical gradient of the oceanic tracers exceeds a given value (Brainerd and Gregg 1995; Lorbacher et al. 2006). The difference criterion largely depends on the difference value chosen and produces misrepresentation of the MLD in regions of weakly stratified surface layers. The gradient criteria also depend on the threshold value chosen for the derivative, but since the gradient is expected to be large at the base of the MLD, it gives more accurate estimations of MLD. Lorbacher et al. (2006) further developed the gradient criteria by adding the standard deviation threshold to assume the shallowest extreme curvature. As a first guess, the nearest MLD is assumed at the local maximum/minimum of the second derivative of the gradient and where the gradient exceeds 0.25 of gradient maximum of the profile. As a secondary boundary condition, 30-m standard deviation (>0.02) is included to distinguish the near-homogeneous region and a standard deviation of gradient over the upper level is then set (0.004 km^{-1} for high and 0.002km^{-1} for low resolution). A more accurate estimation of MLD is provided by an exponential interpolation method (for thick layers), and hence the Lorbacher et al. (2006) criteria is used to estimate the mixed layer from the density profiles for all the data in this study. The results in this paper also hold when difference criteria are used for estimating MLD. We checked with difference in density of 0.03 kg/m^3 and variable density criteria (Montégut et al. 2004) that results shallower or deeper ML than that obtained by Lorbacher et al, (2006). However, the spatial pattern remain fairly similar for all the criteria.

3. Observed MLD

As a starting point for the analysis the seasonal mean MLD estimated from GECCO2 are presented in Fig. 1 (left column). They are largely consistent with those found in previous studies (Kara et al. 2003; Montégut et al. 2004; Lorbacher et al. 2006). Fig. 2 simplifies the seasonal mean MLDs to the annual mean and the relative strength of the seasonal cycle. They show a number of well-known characteristics, such as the strong seasonal cycle in the extra-tropical regions or the shallow MLDs in the upwelling regions along coastlines and the equatorial Pacific. Overall the structure of the global ocean seasonal mean MLD is fairly

238 complex. To simplify the following discussions and analyses it is useful to define some basic
239 MLD regimes, based on the annual mean MLD and the relative strength of the seasonal cycle
240 (Fig. 2). The regime selection criteria where somewhat guided by a good presentation of the
241 following analysis. In terms of MLD the global ocean can be split into the following three
242 regimes:

243 • **Extra-tropical-seasonal**: Regions where the standard deviation of the seasonal cycle
244 is larger than 60% of the annual mean MLD (Fig. 3a). The criteria (60%) cover the
245 regions where significant seasonal variability occurs. These are regions with a very
246 shallow warm-season MLD and a substantially deeper cold-season MLD. This is
247 mostly found in a band along 30-40 degrees with some regions extending further to
248 higher latitudes. The most extreme seasonality is seen in the Southern Ocean in the
249 Indian and Pacific sections, which are within the Antarctic Circumpolar Current
250 (ACC) (Sallée et al. 2006; Dong et al. 2008). The far northern Atlantic is also a region
251 of extreme seasonality.
252 • **Constant-deep**: Regions with an annual mean MLD > 30m and a standard deviation
253 of the seasonal cycle that is less than 60% of the annual mean MLD (Fig. 3b). The
254 30m selection criteria roughly mark half-standard-deviation away from the global
255 mean MLD. These are mostly the off-equatorial tropical and subtropical regions, but
256 also large fractions of the Southern Ocean and parts of the far northern Pacific.
257 • **Constant-shallow**: Regions with an annual mean MLD < 30m and a standard
258 deviation of the seasonal cycle that is less than 60% of the annual mean MLD (Fig.
259 3c). These mark mostly coastal regions and in particular upwelling regions along
260 major continents and equatorial regions, but also coastlines in the north-western North
261 Atlantic and west of Australia. Most of the North Indian Ocean falls in this shallow
262 regime. But in NCEP-GODAS much of the North Indian Ocean falls in the constant-
263 deep regime. It should be noted that MLD in NCEP-GODAS (annual mean is ~52m)
264 is deeper than the other two reanalyses data (~41m in GECCO2 and SODA). The
265 difference could be associated with different model assimilation procedures (Kröger
266 et al. 2012).

267 The following analysis focuses on how these different mean MLD regimes relate to the local
268 atmospheric forcing and the stratification of the upper ocean.
269

270 **3.1 The annual mean MLD and its relationship with local forcing**

The external forces that act on the MLD are the heat, momentum and evaporation-precipitation difference (E-P) fluxes. All these forces interact with and influence the upper-ocean stratification. Strongly stratified profiles require strong forcing to break the stratification and to promote deepening of the mixed layer (ML). A comparison of the annual mean values of the atmospheric forcings and the upper-ocean stratifications (Fig. 4) with the annual mean MLD (Fig. 2a) gives some idea of the relative importance of the different forcings. Note that the shading in Fig. 4 is coded in such a way that bluish colours indicate forcings or stratifications that would support deeper mixed layers, and reddish colours indicate forcings or stratifications that would support shallower MLD.

The annual mean net heat flux (NHF) in the higher latitudes (>40º) is mostly negative, which implies that the ocean is losing heat (Fig 4a). Heat loss at the surface makes the upper ocean statically unstable, which tends to deepen the ML. The upwelling regions along the coastlines and the equator and in the tropical Indian Ocean are marked by annual mean heat gain, which tends to support shallow MLD. Overall there is only a moderate match between the annual mean NHF forcing and the MLD (spatial correlation of -0.3). Most of the *constant-shallow* MLD regime seems to be associated with annual mean heat gain. Also many of the extra-tropical regions with deeper annual mean MLD are associated with corresponding heat loss. However, many regions with shallower than global mean MLD are associated with annual mean heat loss, which does not support the observed shallow MLD (e.g. coastal regions in the western North Pacific and Atlantic and southern subtropical regions in the Indian and Pacific Oceans). Also regions with deeper than global mean MLD are associated with annual mean heat gain, which does not support the observed deep ML (e.g. off-equatorial tropical Pacific and parts of the Southern Ocean).

The annual mean wind-stress forcing (Fig. 4b) shows a slightly better match to the annual mean MLD than NHF (spatial correlation of 0.4). In particular, higher-latitude regions with deep annual mean ML are associated with strong mean wind-stress and equatorial regions with shallow annual mean MLD are associated with weak mean wind-stress. However, there are also large regions where the annual mean MLD is deep despite fairly moderate annual mean wind-stress (e.g. latitude bands around 30 degrees in both hemispheres) and regions where the annual mean MLD is shallow despite fairly strong annual mean wind-stress (e.g. subtropical South Indian Ocean and the Arabian Sea). One can also notice that for most regions NHF and wind-stress have similar influences on the MLD, with both either supporting deeper ML (e.g. most extra-tropical regions) or supporting shallower ML (e.g.

equatorial regions). Notable exceptions here are parts of the subtropical regions, parts of the Southern Ocean, the far northern Pacific, the western North Atlantic and the Arabian Sea.

The precipitation and evaporation (E-P) plays in general a minor role in mixing processes in the upper ocean by changing the density structure (Dong et al. 2009), which is also highlighted here by the mismatch of the annual mean E-P (Fig. 4d) with the annual mean MLD for most regions (spatial correlation of 0.0). The mean E-P forcing is also mostly unrelated to the NHF and wind-stress forcings. In some regions, however, where both NHF and wind-stress forcings do not match the MLD, the E-P forcing does indeed seem to match the MLD. These appear to be mostly smaller and coastal regions (e.g. coastal regions of Greenland and some parts of the western boundary of the North Pacific and Atlantic).

Remarkable are the shallower MLD regions in the subtropical Indian and western Pacific Oceans. Here, all three atmospheric forcings would support deeper annual mean MLD. The shallower MLDs here seem to match the stronger upper-ocean stratifications, displayed in Fig. 4c (spatial correlation of -0.5) in terms of the density gradient between the surface and 100m depth. Although, upper-ocean stratification is partly a reflection of the atmospheric forcings, it is also influenced by oceanic processes. Since the annual mean atmospheric forcings seem to mismatch the mean MLD in these regions, it suggests that oceanic processes independent of the local atmospheric forcing contribute to the stratification of the upper ocean and thus a shallower MLD.

3.2 The MLD seasonal cycle and its relationship with local forcing

The *extra-tropical-seasonal* MLD regime largely represents the world ocean regions with strong mean MLD seasonal cycle (Fig. 2b). These regions are fairly well matched with the strength of the NHF seasonal cycle (Fig. 5a) with a spatial correlation of ~0.6. Although the wind-stress forcings in the Northern Hemisphere support the *extra-tropical-seasonal* MLD regime, they do not show strong seasonality in the Southern Hemisphere (Fig. 5b). Thus it seems that the *extra-tropical-seasonal* MLD regime is mostly a result of seasonally varying tendencies of heating and cooling at the surface. This is consistent with previous findings (Monterey and Levitus, 1997; Kara et al. 2003; Montégut et al. 2004). Also, seasonal variability in density gradients (Fig 5c) and E-P (Fig 5d) shows only a moderate match (spatial correlation of 0.3 and -0.2 respectively) with the seasonality in MLD. However, again there are some regions where this simple picture is not supported. In particular, the western boundaries of the North Pacific and Atlantic have a very strong seasonal cycle in NHF, but

not in the MLD. Also the very strong seasonality in the Indian and Pacific Oceans' ACC regions are not directly matched by the seasonality in either of the atmospheric forcings.

An interesting aspect of the combined effect of annual mean forcing and the strength of the seasonality in the forcings can be seen along the zonal bands in the northern midlatitudes (Fig. 6). In the zonal band at around 30^{o}N in the North Pacific the MLD is deeper on the western side and it has a stronger seasonality. Both mean and seasonality decrease to the east. This is supported by the behaviour of the mean heat flux and its seasonality. In the west an annual mean cooling and strong seasonality support the MLD behaviour; to the east the mean cooling turns into a mean warming and the seasonality in NHF decreases, again supporting the MLD behaviour. This reflects the change in atmospheric forcing from having strong continental characteristics in the west (e.g. strong cooling in winter and strong seasonality) and being more in balance with the ocean state in the east, due to the preferred westerly wind conditions that tend to transport characteristics from the west to the east. This is somewhat similar in the North Atlantic, but the relationship breaks down near the western boundary region.

3.3 Anomaly variability and its relationship with local forcing

Next, it is interesting to regard the MLD variability beyond the seasonal cycle. The second column of Fig. 1 shows the standard deviation (stdv) of monthly mean MLD anomalies estimated for each season. The patterns of strong and weak MLD stdv match very well the patterns of deep and shallow mean MLD (first column in Fig. 1). Thus, MLD variability is stronger when the mean MLD is deep and MLD variability is weak when the mean MLD is shallow. This pattern even holds when we consider the coefficient of variance (CV; the ratio of stdv over the mean) as shown in the last column of Fig. 1. The equatorial Pacific and Atlantic, however, mark regions where the MLD variability is strong even though the mean MLD is fairly shallow, which is consistent with the study by Lorbacher et al. (2006). In these regions the concept of MLD may not be so useful, as they are more dominated by lateral ocean wave dynamics in the thermocline. It is also remarkable to note that a CV > 100% is observed in the spring and winter seasons in the higher latitudes of North Atlantic and Pacific and in the Southern Ocean. This suggests a substantial amount of MLD variability. For most other regions the CV values are larger than 30%, indicating significant MLD variability for most regions in most seasons. Keerthi et al. (2012) have also shown large CV values (>40%) in the western and eastern equatorial Indian Ocean during boreal summer.

Fig. 7 shows the cross-correlation between monthly mean MLD and NHF anomalies in-phase and with one-month lead-time for the NHF for different seasons. Negative in-phase correlations dominate in all seasons and most regions, consistent with cooling (negative NHF anomalies) at the surface ocean leading to increased convective mixing and, hence, a deeper ML; and vice versa for positive NHF anomalies. Equatorial regions in the central Pacific and western Atlantic, however, show negligible correlation between NHF and MLD anomalies. Further, the in-phase correlation in both hemispheres (in the midlatitudes) is stronger in fall and winter and fairly weak in spring and summer. The one-month MLD lag cross-correlation with NHF is largest in the fall season and weakest in the spring season in both hemispheres. This relation is consistent with the idea that deeper MLDs evolve more slowly and therefore have a longer lag-time relation between forcing (NHF) and MLD anomaly.

The wind-stress forcing is in most regions positively correlated with MLD, consistent with stronger than normal wind-stress anomalies leading to deeper MLDs, and vice versa for negative wind-stress anomalies (Fig. 8). In the mid to higher latitudes this relationship tends to be stronger in spring and summer. The strongest correlations are essentially found in two regions: the off-equatorial tropical and subtropical regions with a tendency for stronger correlations in the warmer season, and the extra-tropical higher latitudes in the Southern Ocean and to a smaller extent in the far northern Pacific and Atlantic. The lag one-month correlation overall appears to be strongest in the subtropical regions and in the fall season in the Southern Ocean.

The cross-correlations of MLD with both NHF and wind-stress are mostly on a similar level, with some more widespread and clearer correlation for the NHF with MLD. Cross-correlations of MLD with E-P are in general weaker than those with NHF and wind-stress, but are mostly positive, which is consistent with increased evaporation (salinity forcing) leading to deeper MLs (see SFig. 1). This relationship is strongest in fall and winter seasons in both hemispheres.

4. The ACCESS-KPP model

We now take a look at the MLD and its relation to the atmospheric forcings in the ACCESS-KPP model with a single-column ocean mixed layer model. Thus, in this model the simulated MLD is purely a result of local atmospheric forcing, vertical mixing and a heat and salinity flux correction, which is independent of the background state, to prevent the model from drifting away from the observed mean density profiles.

A comparison of the patterns of the seasonal mean MLDs and its variability between observations (Fig. 1) and the ACCESS-KPP model (Fig. 9) already illustrates that the model represents the mean MLD characteristics very well. In the following, the same MLD characteristics as above for observations will be analysed in the ACCESS-KPP model. Further the role of the flux corrections in maintaining the realistic upper-ocean density profiles will be investigated.

4.1 The annual MLD and its relationship with local forcing

The figures 10 and 11 show the same atmospheric forcings and upper-ocean stratification fields as in figures 4 and 5, but for the ACCESS-KPP model. First of all one can notice that the annual mean and seasonal cycle of the atmospheric forcings in the ACCESS-KPP model are very similar to the observed values (spatial correlations are greater than 0.7, see Table 1 in the supplementary material). This suggests that the MLD characteristics in the ACCESS-KPP model can be analysed for similar atmospheric forcings conditions. Some mismatches exist in the annual mean NHF in the northern Indian Ocean and tropical north Atlantic, where the observed NHF is positive but the ACCESS-KPP model values are negative. However, there are also some differences in these characteristics among the ocean reanalysis products (see Table 2 in the supplementary material for spatial correlation between the ocean reanalysis products), suggesting that such differences are not necessarily an indication of a significant model bias.

The regional distribution of the annual mean MLD and the three main MLD regimes in the ACCESS-KPP model are fairly similar to the observed (compare Figs. 12 and 13 with 2 and 3). The ACCESS-KPP model has a very similar regional distribution of the *extra-tropical-seasonal* MLD regime, it also simulates the *constant-deep* MLD regime with a subtropical and Southern Ocean region and it simulates parts of the *constant-shallow* MLD regime in the coastal upwelling regions. However, some significant differences between the ACCESS-KPP model and the observations can be noted: first, the overall mean MLD in the ACCESS-KPP model is deeper than observed (63m and 41m, respectively). Here it should be noted that annual mean in the other ocean reanalysis product NCEP-GODAS is ~52m and for SODA it is ~41m. It must however be kept in mind that MLD in the model is predominantly driven by the atmospheric forcing; the strong inclination of ML dynamics on atmospheric forcing could be a reason for relatively deeper ML in the model. The model also misses several regions within the *constant-shallow* MLD regime: the equatorial cold tongues, the tropical Indian Ocean and the northern oceans coastal regions. The model's *extra-tropical-seasonal* MLD

regime is also slightly more widespread in the northern oceans than observed. Further, the ACCESS-KPP model simulates fairly deep ML in the eastern subtropical Pacific and subtropical Indian Ocean, which is much shallower in the observations. The deeper ML in these regions seems to fit to fairly strong annual mean local atmospheric heat and wind forcings. It thus seem to indicate that the observed shallow ML in these regions does not result from the local forcing, but may involve interactive lateral ocean dynamics not represented in the single-column ACCESS-KPP model. The northern North Atlantic shows deeper MLs in the model despite weak wind forcing compared to the observed. In the model, stronger cooling (compared to the observed) as well as statically less stable upper-ocean (caused by relatively high surface salinity) results in overturning to great depth producing deeper MLs in this region.

The relationship between the atmospheric forcings and the MLD in the ACCESS-KPP model is also similar to the observed (compare Figs. 4 and 10). Again the wind-stress forcing tends to be more strongly related to the annual mean MLD than the heat flux forcing and again the E-P forcing has no relationship with the annual mean MLD.

4.2 The seasonal cycle of MLD and its relationship with local forcing

As stated above, the model is able to reproduce the observed seasonal changes reasonably well (compare Figs 2b and 12b): it essentially captures the zonal bands of the strong *extra-tropical-seasonal* MLD regime in the midlatitudes. Seasonal amplitude is weaker in the tropics, subtropics and also in parts of the Southern Ocean. As already indicated in the previous section, the ACCESS-KPP model tends to overestimate the seasonality in the eastern North Pacific and the western coastal region in the North Atlantic. The model is good at representing the mean summer MLD, but overestimates MLD during fall and spring. This however, cannot be due to stronger seasonality in the atmospheric forcings, as they appear to be similar or weaker than observed. This suggests that the ACCESS-KPP model is missing some ocean dynamics necessary to capture these features.

The seasonal cycle of the atmospheric forcings is well captured by the ACCESS-KPP model and again the relationship between the heating and wind-stress forcings and the MLD are mostly as observed (compare Figs 5 and 11). Thus, the seasonality in the NHF is the main forcing for the seasonal cycle of the MLD in ACCESS-KPP model.

4.3 Anomaly variability and its relationship with local forcing

The overall strength and seasonal distribution of the anomaly variability of the MLD in the ACCESS-KPP model is very similar to the observed (compare Figs. 1 and 9). The stdv of the MLD is mostly strong where the mean ML is deep, but it follows the mean MLD even more closely than observed. Thus, the coefficient of variance is more homogenous in the ACCESS-KPP model.

The correlation between heat flux and wind-stress forcings and the MLD in the model have similar signs as in observations in all seasons, but are overall much stronger (compare Figs. 7 and 8 with 14 and 15). This could be related to both errors in the reanalysis dataset and to the simplified dynamics of the ACCESS-KPP model. The observations include atmospheric heat fluxes, ocean observations and the model simulation of the reanalysis model. Errors in these elements will lead to inconsistencies between the forcings and the MLD. Subsequently, one has to assume that the correlation between forcings and the MLD is decreased in the observations. On the other hand, the ACCESS-KPP model has simplified dynamics that only include local forcings and vertical mixing, neglecting all other lateral ocean dynamics. Subsequently, one has to assume that the correlation between local forcings and the MLD is artificially enhanced.

As in the observations the effect of the anomalous wind stress forcings is stronger in the warmer, shallower MLD seasons. The lag-1 correlation of the heat flux is also stronger in the cold, deep ML seasons as in the observations. The E-P also shows higher correlations with MLD (see SFig.1 and 2) than observed, but still much weaker than the correlations with heat flux and wind stress, suggesting that the E-P forcing is not as important.

4.4 Missing dynamics and the role of flux corrections

Although the ACCESS-KPP model represents the seasonal mean MLD and its variability fairly well by only simulating the local atmospheric forcing and the vertical single column dynamics, it does also have substantial limitations. A key aspect of the ACCESS-KPP model is that additional heat and salt flux correction terms exist on all levels in the ocean model. These flux corrections are essential in many regions to maintain the overall stratification in the density profile of the ocean, see Fig. 16(a,b). Without in particular the heat flux corrections (salinity corrections not shown), the ocean stratification in the tropics and subtropics would collapse eventually (over periods longer than 10 years) and the warm surface waters would mix all the way to the bottom layer of the KPP model (1000m depth). This is indicated by the significant surface warming and subsurface cooling effect of the heat flux correction over wide spread regions in the tropics and subtropics. This effectively

stabilizes the density profile and thus maintains the ocean stratification. The flux correction shown in Fig 16a (upper 50m) are of comparable magnitude to the atmospheric heat flux forcing (in Fig 4a). Also, the seasonal variability of heat flux correction in the upper 50m (Fig 16c) is large (no seasonal variability in the subsurface levels, Fig 16d). Since the flux corrections mimic the mean effect of the missing ocean dynamics, it suggests that interactive lateral ocean dynamics not simulated in the ACCESS-KPP model are also important for simulating the main MLD characteristics.

5. Summary and Discussion

In this study, the spatial and temporal relationship between the local atmospheric forcing and the mean, seasonal cycle and variability of the MLD are analysed using a recent ocean reanalysis product (GECCO2) and a single-column ocean model (KPP) coupled to an atmospheric GCM (ACCESS1.3) over the global ocean. The aim of this study was to understand the driving mechanisms of the MLD in different regions and to what extent these can be understood in terms of local air-sea interactions. The focus was on the MLD characteristics of the annual mean, the relative seasonal cycle strength and the variability anomalous from the seasonal cycle. To further simplify the fairly complex characteristics three main regimes were introduced based on the characteristics of the annual mean and the relative seasonal cycle strength of the MLD.

First of all, the findings about the annual mean and the relative seasonal cycle strength of the MLD can be summarised as follows:

- The annual mean MLD over most open ocean regions (away from sea ice and shallow coastal regions) follows the wind and heat forcing. Regions with stronger mean wind forcing tend to have larger annual mean MLD and regions with annual mean net heating tend to have shallower annual mean MLD. The annual mean wind forcing strength appears to be most strongly related to the annual mean MLD and stronger than the net heat forcing. Both of these forcing, however, show spatial correlations less than ~0.5 with the global pattern of the annual mean MLD, indicating that the relationship is more complex. The large flux correction needed to prevent model drift signifies that ocean dynamics are also important for simulating MLD.
- Remarkable are a few regions, in which neither of the atmospheric forcings seem to match the annual mean or seasonal cycle characteristics of the MLD. The shallower MLD regions in the subtropical Indian and western Pacific Oceans do not seem to

relate to any of the three atmospheric forcing. The western boundaries of the North Pacific and Atlantic have very strong seasonal cycle in NHF, but not in the MLD. Also, the very strong seasonality in the Indian and Pacific Oceans' ACC regions are not directly related to the seasonality in either of the atmospheric forcings. Since the atmospheric forcings seem to mismatch the MLD characteristics (in the reanalysis datasets) in these regions and the single-column ocean model is also not able to simulate these characteristics, it suggests that oceanic processes independent of the local atmospheric forcing contribute to the stratification of the upper ocean and thus the MLD in significant ways.

- The annual mean E-P forcing is for most regions not related to the annual mean MLD, suggesting it is not a dominating forcing. However, in some regions, where both annual mean NHF and wind-stress tendencies do not match the MLD, the E-P forcing does indeed seem to play a role for the annual mean MLD (e.g. coastal regions of Greenland and some parts of the western boundary of the North Pacific and Atlantic).
- The relative seasonal cycle strength of the MLD is also mostly related to the relative seasonal cycle strength of the net heating and wind stress, but here the relationship with the net heating is stronger than with the wind forcing. Thus, the relative seasonal cycle strength of the MLD mostly follows the strength of the seasonal cycle in the net heating.

Alternatively the processes that dominate the three different MLD regimes can be summarised:

- **Extra-tropical-seasonal**: This regime of the MLD in the midlatitudes is primarily a result of the strong seasonal cycle in the heating. The seasonal cycle in heating is indeed strongest in the midlatitudes and matches the strongest relative seasonal cycle strength of the MLD fairly well. In this regime, however, the atmospheric storm track positions also play a major role as well as oceanic fronts and strong boundary currents that are not simulated in the model.
- **Constant-deep**: The regime, where the ML is fairly deep (>30m) throughout the year with no strong seasonal cycle, is mostly found in the subtropics and some high latitudes. These are regions with no strong annual mean heating nor cooling, no strong seasonal cycle in heating and the winds tend to be slightly less than the global mean.
- **Constant-shallow**: Shallow MLDs without strong seasonal cycles are mostly found in coastal regions, equatorial regions and the tropical Indian Ocean. Some of these

regions are fairly well related to the local forcings, such as coastal and some equatorial upwelling regions. However, much of this *constant-shallow* MLD regime is not well matched with the local forcings and is not well simulated in the ACCESS-KPP simulation, suggesting that local forcings and processes are not sufficient to explain these MLD characteristics. In particular, in the higher latitudes coastal regions, the central ocean basin equatorial regions and in the Indian Ocean the *constant-shallow* MLD regimes are not matched to local forcings or processes.

The analysis of the anomalous variability of MLD and how it relates to the local forcing can be summarised by the following main points:

- The overall strength of the MLD variability is in general proportional to the mean MLD, with stronger variability associated with a deeper mean MLD (e.g. cold season). The MLD variability appears to be quite significant with values of 30% to more than 100% of the seasonal mean MLD values.
- Most of this is well captured by the ACCESS-KPP model, but in some regions this is not well simulated by the model, including the equatorial Pacific. In higher latitudes the model does not simulate as strong MLD variability relative to the seasonal mean MLD as observed.
- MLD variability is mostly negatively correlated with heat flux variability and positively with wind stress variability. In the mid to higher latitudes the relationship to heating tends to be stronger in the cold (deep ML) seasons and the relationship to wind forcing tends to be stronger in the shallower MLD (warm) seasons. In seasons with deeper mean MLD the relationship to the atmospheric forcings tends to become stronger when the atmospheric forcings lead by about one month, which seems to be consistent with a larger inertia of the MLD when it is deeper.
- The ACCESS-KPP model is consistent with these observed relationships between the local atmospheric forcings and the MLD, but the relationships are significantly stronger in the model simulations. This may to some part reflect the simplification of the model to only local vertical mixing processes and neglecting other ocean dynamics, which leads to an overestimate of the role of local forcings on the MLD variability. But it may also point to errors in the reanalysis datasets that lead to inconsistencies between atmospheric forcings and the ocean state that artificially degrade the relationship between local forcing and the MLD.

While overall the local forcing perspective provides a fairly good representation of most of the MLD characteristics in the global oceans, it does have some limitations as mentioned above. This is in particular highlighted by the fact that the ACCESS-KPP model does require significant flux correction in temperature (most importantly) and also in salinity. These are important to maintain upper-ocean stratification close to observations. Without such terms in the ACCESS-KPP model, the upper-ocean stratification in most subtropical regions would collapse after about 10 years and the MLD would deepen to the base of the ACCESS-KPP model (1000m). Thus, with the flux correction terms, the coupled single-column model allows to study the upper ocean-atmosphere interaction with higher near-surface vertical resolution incorporated with a better vertical mixing. This coupled framework is computationally less expensive and allows identification of the role of atmospheric forcings for the upper-ocean processes.

The analysis has shown that the MLD characteristics arise from complex interactions between the local forcings, ocean stratifications and potentially lateral ocean dynamics. Most of the results discussed here result from comparisons of the overall statistics of MLD and local forcings in observations and in the ACCESS-KPP simulation. To further untangle the interactions and the relative contribution of different forcings and different oceanic processes it would require sensitivity experiments with the ACCESS-KPP or similar model simulations, in which forcings or elements of the forcings are turned 'off' or in which processes are altered or turned 'off'. However, this is beyond this study and is left for future analyses.

Acknowledgments

The authors would like to thank Australian National Computational Infrastructure, in Canberra, for providing computational platform for simulation of the ACCESS-KPP coupled model. The ARC Climate System Science (CE110001028) supported this study. Nicholas Klingaman was funded by the National Centre for Atmospheric Science-Climate, a collaborative centre of the Natural Environment Research Council, under agreement R8/H12/83/001.

631 **Reference**

632

633 Adamec D, Elsberry RL (1984) The use of mean atmospheric forcing in an ocean mixed-
634 layer model. Journal of Physical Oceanography 14:1670-1676

635

636 Alexander M, Scott J, Deser C (2000) Processes that influence sea surface temperature and
637 ocean mixed layer depth variability in a coupled model. Journal of Geophysical Research
638 105:16823. doi: 10.1029/2000JC900074

639

640 Antonov JI, Seidov D, Boyer TP, Locarnini RA, Mishonov AV, Garcia HE, Baranova OK,
641 Zweng MM, Johnson DR (2010) World Ocean Atlas 2009, Volume 2: Salinity. S. Levitus,
642 Ed. NOAA Atlas NESDIS 69, U.S. Government Printing Office, Washington, D.C., 184 pp.

643

644 Bates N (2001) Interannual variability of oceanic CO2 and biogeochemical properties in the
645 Western North Atlantic subtropical gyre. Deep Sea Research Part II: Topical Studies in
646 Oceanography 48:15071528. doi: 10.1016/S0967-0645(00)00151-X

647

648 Behringer DW, Xue Y (2004) Evaluation of the global ocean data assimilation system at
649 NCEP: The Pacific Ocean. Eighth Symposium on Integrated Observing and Assimilation
650 Systems for Atmosphere, Oceans, and Land Surface. Washington State Convention and
651 Trade Center, Seattle, Washington, pp 11–15

652

653 Bi D, Dix M, Marsland SJ, et al (2013) The ACCESS coupled model: description, control
654 climate and evaluation. Australian Meteorological and Oceanographic Journal 63:41–64.

655

656 Brainerd KE, Gregg MC (1995) Surface mixed and mixing layer depths. Deep Sea Research
657 Part I: Oceanographic Research Papers 42:1521–1543. doi: 10.1016/0967-0637(95)00068-H

658

659 Carton J, Grodsky S, Liu H (2008) Variability of the Oceanic Mixed Layer, 1960–2004.
660 Journal of Climate 21:10291047. doi: 10.1175/2007JCLI1798.1

661

662 Carton J, Giese B (2008) A Reanalysis of Ocean Climate Using Simple Ocean Data
663 Assimilation (SODA). Mon Wea Rev 136:29993017. doi: 10.1175/2007MWR1978.1

664

Chen D, Busalacchi A, Rothstein L (1994) The roles of vertical mixing, solar radiation, and wind stress in a model simulation of the sea surface temperature seasonal cycle in the tropical Pacific Ocean. Journal of Geophysical Research: Oceans 99:20345–20359. doi: 10.1029/94JC01621

Cronin M, Kessler W (2002) Seasonal and interannual modulation of mixed layer variability at 0°, 110°W. Deep Sea Research Part I: Oceanographic Research Papers 49:117. doi: 10.1016/S0967-0637(01)00043-7

Dommenget D, Latif M (2002) Analysis of observed and simulated SST spectra in the midlatitudes. Climate Dynamics 19:277–288. doi: 10.1007/s00382-002-0229-9

Dommenget D, Latif M (2008) Generation of hyper climate modes. Geophysical Research Letters. doi: 10.1029/2007GL031087

Dong S, Gille S, Sprintall J (2007) An Assessment of the Southern Ocean Mixed Layer Heat Budget. J Climate 20:4425-4442. doi: 10.1175/JCLI4259.1

Dong S, Sprintall J, Gille S, Talley L (2008) Southern Ocean mixed-layer depth from Argo float profiles. Journal of Geophysical Research: Oceans. doi: 10.1029/2006JC004051

Dong S, Garzoli S, Baringer M (2009) An assessment of the seasonal mixed layer salinity budget in the Southern Ocean. J Geophys Res. doi: 10.1029/2008JC005258

Fasham M (1995) Variations in the seasonal cycle of biological production in subarctic oceans: A model sensitivity analysis. Deep Sea Research Part I: Oceanographic Research Papers 42:1111-1149. doi: 10.1016/0967-0637(95)00054-A

Godfrey J, Lindstrom E (1989) The heat budget of the equatorial western Pacific surface mixed layer. J Geophys Res 94:8007–8017. doi: 10.1029/JC094iC06p08007

696 Halkides D, Lee T (2009) Mechanisms controlling seasonal-to-interannual mixed layer
697 temperature variability in the southeastern tropical Indian Ocean. J Geophys Res. doi:
698 10.1029/2008JC004949
699
700 Hirons L, Klingaman N, Woolnough S (2015) MetUM-GOML1: a near-globally coupled
701 atmosphere–ocean-mixed-layer model. Geosci Model Dev 8:363–379. doi: 10.5194/gmd-8-
702 363-2015
703
704 Kantha L, Clayson C (1994) An improved mixed layer model for geophysical applications.
705 Journal of Geophysical Research: Oceans 99:25235–25266. doi: 10.1029/94JC02257
706
707 Kantha, L, Clayson C (2000) Small scale processes in geophysical fluid flows. International
708 Geophysics Series, vol. 67. Academic Press, New York, pp 157-160.
709
710 Kara BA, Rochford P, Hurlburt H (2000) An optimal definition for ocean mixed layer depth.
711 J Geophys Res 105:16803–16821. doi: 10.1029/2000JC900072
712
713 Kara BA, Rochford P, Hurlburt H (2003) Mixed layer depth variability over the global ocean.
714 J Geophys Res 108:3079. doi: 10.1029/2000JC000736
715
716 Keerthi M, Lengaigne M, Vialard J, et al (2012) Interannual variability of the Tropical Indian
717 Ocean mixed layer depth. Climate Dynamics 40:743–759. doi: 10.1007/s00382-012-1295-2
718
719 Klingaman N, Woolnough S (2014) The role of air–sea coupling in the simulation of the
720 Madden–Julian oscillation in the Hadley Centre model. QJR Meteorol Soc 140:2272–2286.
721 doi: 10.1002/qj.2295
722
723 Köhl A (2014) Evaluation of the GECCO2 ocean synthesis: transports of volume, heat and
724 freshwater in the Atlantic. Quarterly Journal of the Royal Meteorological Society. doi:
725 10.1002/qj.2347
726
727 Kröger J, Müller W, Storch J-S (2012) Impact of different ocean reanalyses on decadal
728 climate prediction. Clim Dyn 39:795–810. doi: 10.1007/s00382-012-1310-7

729
730 Large WG, McWilliams JC, Doney SC (1994) Oceanic vertical mixing: A review and a
731 model with a nonlocal boundary layer parameterization. Reviews of Geophysics 32:363–403.
732 doi: 10.1029/94RG01872
733
734 Large WG, Crawford GB (1995) Observations and simulations of upper ocean response to
735 wind events during the Ocean Storms Experiment. Journal of Physical Oceanography
736 25:2831–2852
737
738 Locarnini RA, Mishonov AV, Antonov JI, Boyer TP, Garcia HE, Baranova OK, Zweng MM,
739 Johnson DR (2010) World Ocean Atlas 2009, Volume 1: Temperature. S. Levitus, Ed.
740 NOAA Atlas NESDIS 68, U.S. Government Printing Office, Washington, D.C., 184 pp.
741
742 Lorbacher K, Dommenget D, Niiler P, Köhl A (2006) Ocean mixed layer depth: A subsurface
743 proxy of ocean-atmosphere variability. Journal of Geophysical Research: Oceans. doi:
744 10.1029/2003JC002157
745
746 Maykut G, McPhee M (1995) Solar heating of the Arctic mixed layer. J Geophys Res
747 100:24691–24703. doi: 10.1029/95JC02554
748
749 Montégut C, Madec G, Fischer A, et al (2004) Mixed layer depth over the global ocean: An
750 examination of profile data and a profile-based climatology. Journal of Geophysical
751 Research: Oceans. doi: 10.1029/2004JC002378
752
753 Montégut C, Mignot J, Lazar A, Cravatte S (2007) Control of salinity on the mixed layer
754 depth in the world ocean: 1. General description. Journal of Geophysical Research: Oceans.
755 doi: 10.1029/2006JC003953
756
757 Monterey G, Levitus S (1997) Seasonal Variability of Mixed Layer Depth for the World
758 Ocean, NOAA Atlas NESDIS 14:100 p, Natl. Oceanic and Atmos. Admin., Silver Spring,
759 Md
760
761 Narvekar J, Kumar S (2006) Seasonal variability of the mixed layer in the central Bay of

762 Bengal and associated changes in nutrients and chlorophyll. Deep Sea Research Part I:
763 Oceanographic Research Papers 53:820-835. doi: 10.1016/j.dsr.2006.01.012
764
765 Peter A, Hénaff M, Penhoat Y, et al (2006) A model study of the seasonal mixed layer heat
766 budget in the equatorial Atlantic. J Geophys Res. doi: 10.1029/2005JC003157
767
768 Polovina J, Mitchum G, Evans G (1995) Decadal and basin-scale variation in mixed layer
769 depth and the impact on biological production in the Central and North Pacific, 1960-88.
770 Deep Sea Research Part I: Oceanographic Research Papers 42:1701–1716. doi:
771 10.1016/0967-0637(95)00075-H
772
773 Qui B, Chen S, Hacker P (2004) Synoptic-Scale Air–Sea Flux Forcing in the Western North
774 Pacific: Observations and Their Impact on SST and the Mixed Layer. Journal of Physical
775 Oceanography 34:2148–2159. doi: 10.1175/1520-0485(2004)034<2148:SAFFIT>2.0.CO;2
776
777 Sabine CL, Feely RA, Gruber N, et al (2004) The oceanic sink for anthropogenic CO2.
778 Science 305:367–71. doi: 10.1126/science.1097403
779
780 Sallée JB, Wienders N, Speer K, Morrow R (2006) Formation of subantarctic mode water in
781 the southeastern Indian Ocean. Ocean Dynamics 56:525-542. doi: 10.1007/s10236-005-0054-
782 x
783
784 Swenson M, Hansen D (1999) Tropical Pacific Ocean Mixed Layer Heat Budget: The Pacific
785 Cold Tongue. J Phys Oceanogr 29:69-81. doi: 10.1175/1520-
786 0485(1999)029<0069:TPOMLH>2.0.CO;2
787
788 Takahashi T, Feely R, Weiss R, et al (1997) Global air-sea flux of CO2: An estimate based
789 on measurements of sea–air pCO2 difference. Proceedings of the National Academy of
790 Sciences 94:8292–8299. doi: 10.1073/pnas.94.16.8292
791
792

Figure Captions

Fig 1: Seasonal statistics of MLD estimated from GECCO2 density profiles averaged over January-March (a,b,c), April-June (d,e,f), July-September (g,h,i) and October-December (j,k,l) for the period 1948-2011. The left column shows the seasonal mean MLD (a,d,g,j). The standard deviations of the MLD calculated for each calender month and then seasonally averaged are shown in the middle column (b,e,h,k). The right column (c,f,i,l) shows the seasonal average of the monthly standard deviation relative to the corresponding monthly mean MLD (i.e., the coefficient of variance).

Fig 2: (a) Annual mean MLD estimated from GECCO2 density profiles (30m contour represents shallow mixed layer), and (b) Seasonal amplitude (computed as the standard deviation of the monthly climatology) of MLD relative to the annual mean MLD and the contour represents 60% variability.

Fig 3: Different MLD regimes based on GECCO2 dataset: (a) Extra-tropical-seasonal; regions where seasonal amplitude change is >60% of the annual mean MLD. (b) Constant-deep; regions where MLD >30m and seasonal change is <60%. (c) Constant-shallow; regions with <60% relative seasonal change and MLD <30m.

Fig 4: GECCO2 annual mean fields: (a) Net heat flux (NHF); positive/negative sign indicates the ocean is gaining/losing heat, (b) wind-stress, (c) density gradient (kg/m^4) between the surface and 100m depth, and (d) evaporation minus Precipitation (E-P). Colour code is in such a way that blue shading represents favourable for deep MLD and red shading for shallow mixed layers. Spatial correlation (r) between the forcing variable and the annual mean MLD (Fig 2a) is shown at the top left corner of the corresponding subplot.

Fig 5: Seasonal amplitude of GECCO2 variables (computed as the standard deviation of the monthly climatology): (a) Net heat flux (NHF), (b) wind-stress, (c) density gradient (kg/m^4) between the surface and 100m depth, and (d) evaporation minus Precipitation (E-P). Spatial correlation (r) between the seasonal change of the forcing variable and the MLD (relative to the annual mean as in Fig 2b) is shown at the top left corner of the corresponding subplot.

Fig 6: The annual mean MLD, net heat flux (NHF) and wind-stress (from GECCO2) averaged along (a) 30º-32ºN (North Pacific) and (b) 33º-35ºN (North Atlantic). The positive/negative heat flux (NHF) values indicate that the ocean is losing/gaining heat. The coloured shading represents the corresponding seasonal amplitude change at each grid point (light red for NHF, light blue for MLD and light yellow is for wind-stress).

Fig 7: Cross correlation of net heat flux (NHF) and MLD anomalies in different seasons from GECCO2. Left column shows concurrent correlations and the right column represents the corresponding one-month lag correlations, where MLD lags the forcing by one month. The rows represent from top to bottom the different seasons: January-March (JFM), April-June (AMJ), July- September (JAS), and October-November (OND). Significant (95%) non-zero correlation value is ±0.1.

Fig 8: Cross correlation of wind stress (TAU) and MLD anomalies in different seasons from GECCO2. Left column shows concurrent correlations and the right column represents the corresponding one-month lag correlations, where MLD lags the forcing by one month. The rows represent from top to bottom the different seasons: January-March (JFM), April-June (AMJ), July- September (JAS), and October-November (OND). Significant (95%) non-zero correlation value is ±0.1.

Fig 9: Seasonal statistics of MLD as in Fig 1 but for the ACCESS-KPP coupled model.

Fig 10: ACCESS-KPP annual mean fields (same as in Fig 4). Spatial correlation (r) between the forcing variable and the annual mean MLD (in Fig 12a) is shown at the top left corner of the corresponding subplot.

Fig 11: Seasonal amplitude of ACCESS-KPP forcing variables (same as in Fig 5). Spatial correlation (r) between the seasonal change of the forcing variable and the MLD (relative to the annual mean as in Fig 12b) is shown at the top left corner of the corresponding figure.

Fig 12: (a) Annual mean MLD estimated from ACCESS-KPP simulated density profiles (30m contour represents the shallow mixed layer), and (b) Seasonal amplitude of MLD relative to the annual mean MLD, with contour of 60% variability (similar to Fig 2).

Fig 13: Different MLD regimes based on ACCESS-KPP simulation (same as in Fig 3)

Fig 14: Cross correlation of net heat flux (NHF) and MLD anomalies in different seasons as in Fig 7 but for the ACCESS-KPP model. Significant (95%) non-zero correlation value is ±0.1.

Fig 15: Cross correlation of wind-stress (TAU) and MLD anomalies in different seasons as in Fig 8 but for the ACCESS-KPP model. Significant (95%) non-zero correlation value is ±0.1.

Fig 16: Annual mean (a, b) and seasonal cycle (c, d) of heat flux correction applied on the model levels (top) surface to 50m, and (bottom) 200-300m depth. The actual flux correction at each model level is in W/m^3 and here we multiplied with the thickness of all the layers (50m and 100m, respectively) to show the values in units of W/m^2. Seasonal cycle corresponds to the standard deviation of monthly flux correction in W/m^2. The deeper levels have no seasonal cycle corrections.

Supplementary Figure Captions

SFig 1: Cross correlation of E-P and MLD anomalies in different seasons from GECCO2. Left column shows concurrent correlations and the right column represents the corresponding one-month lag correlations, where MLD lags the forcing by one month. The rows represent from top to bottom the different seasons: January-March (JFM), April-June (AMJ), July-September (JAS), and October-November (OND). Significant (95%) non-zero correlation value is ±0.1.

SFig 2: Cross correlation of E-P and MLD anomalies as in SFig 1 but for the ACCESS-KPP coupled model. Significant (95%) non-zero correlation value is ±0.1.

Supplementary Tables

Table 1: Spatial correlation of variables in model and reanalyses data. The hyphen represents missing or no data.

894

895 Table 2: Spatial correlation of variables in GECCO2 and other reanalyses. (The values in
896 brackets are the spatial correlation of GODAS and SODA data). The hyphen represents
897 missing or no data.
898

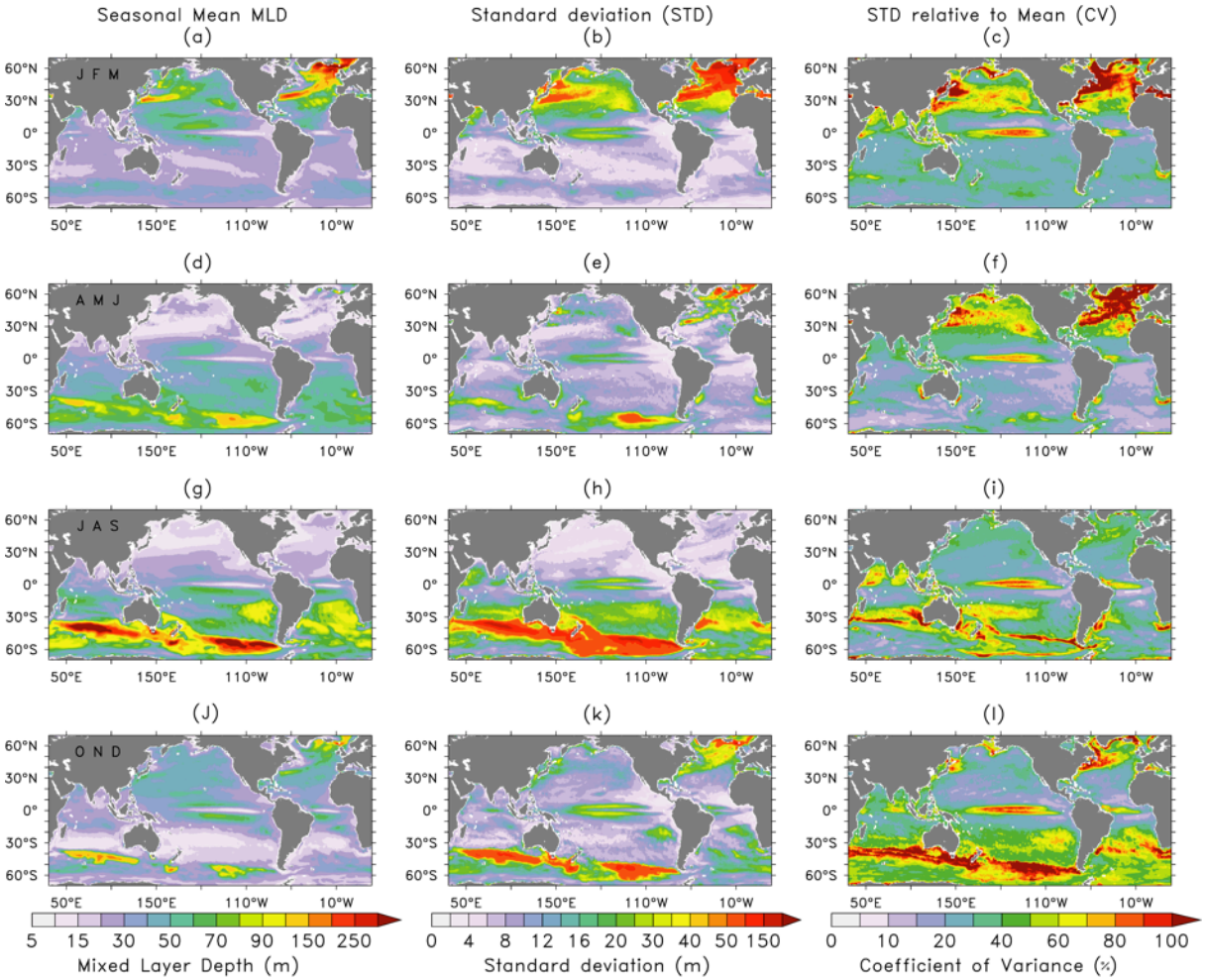

Fig 1: Seasonal statistics of MLD estimated from GECCO2 density profiles averaged over January-March (a,b,c), April-June (d,e,f), July-September (g,h,i) and October-December (j,k,l) for the period 1948-2011. The left column shows the seasonal mean MLD (a,d,g,j). The standard deviations of the MLD calculated for each calender month and then seasonally averaged are shown in the middle column (b,e,h,k). The right column (c,f,i,l) shows the seasonal average of the monthly standard deviation relative to the corresponding monthly mean MLD (i.e., the coefficient of variance).

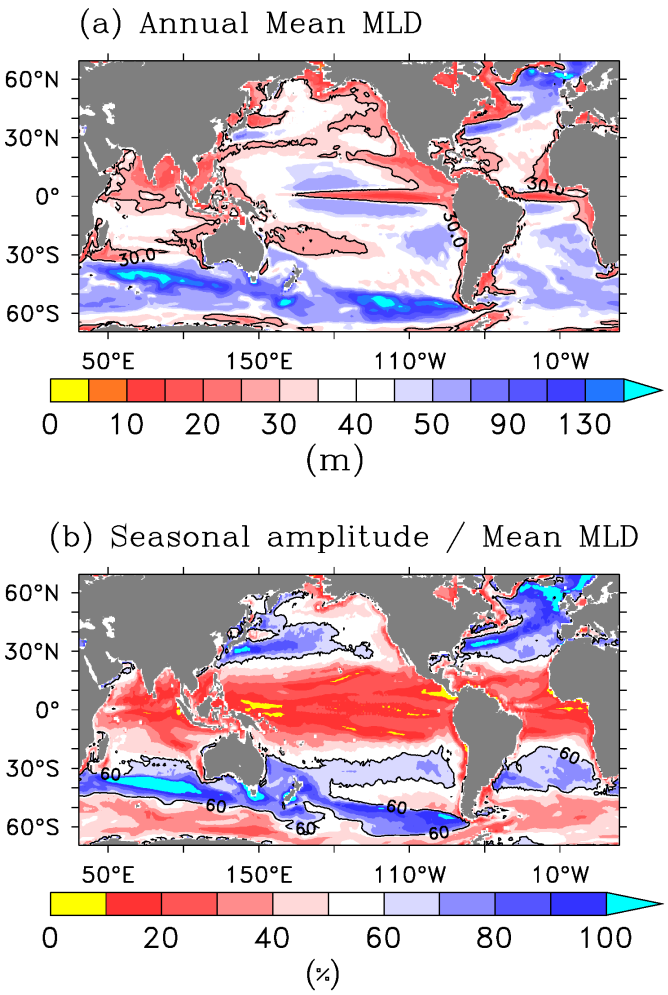

Fig 2: (a) Annual mean MLD estimated from GECCO2 density profiles (30m contour represents shallow mixed layer), and (b) Seasonal amplitude (computed as the standard deviation of the monthly climatology) of MLD relative to the annual mean MLD and the contour represents 60% variability.

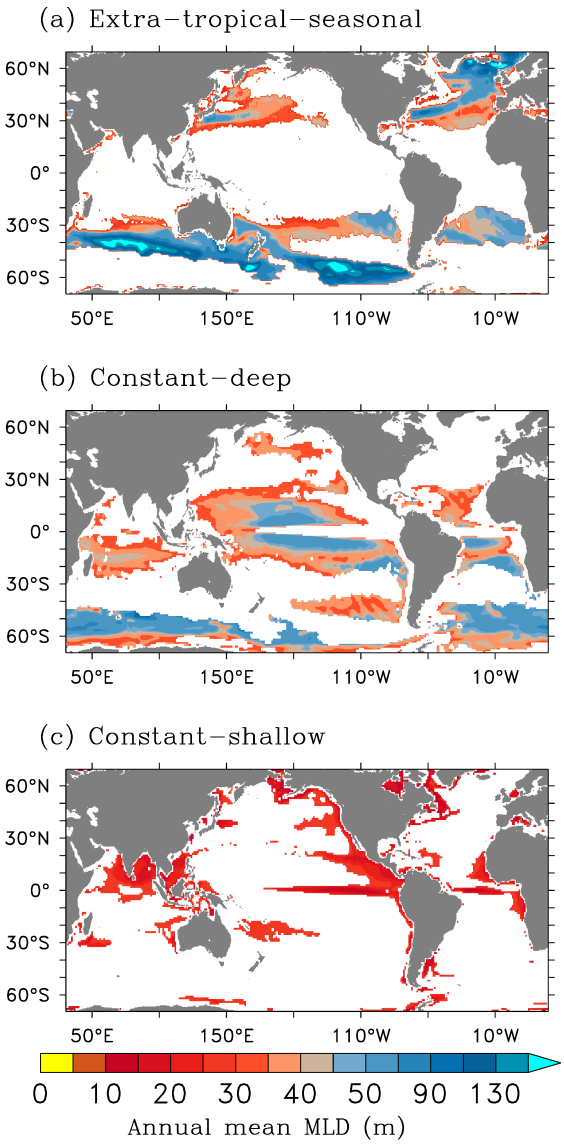

Fig 3: Different MLD regimes based on GECCO2 dataset: (a) Extra-tropical-seasonal; regions where seasonal amplitude change is >60% of the annual mean MLD. (b) Constant-deep; regions where MLD >30m and seasonal change is <60%. (c) Constant-shallow; regions with <60% relative seasonal change and MLD <30m.

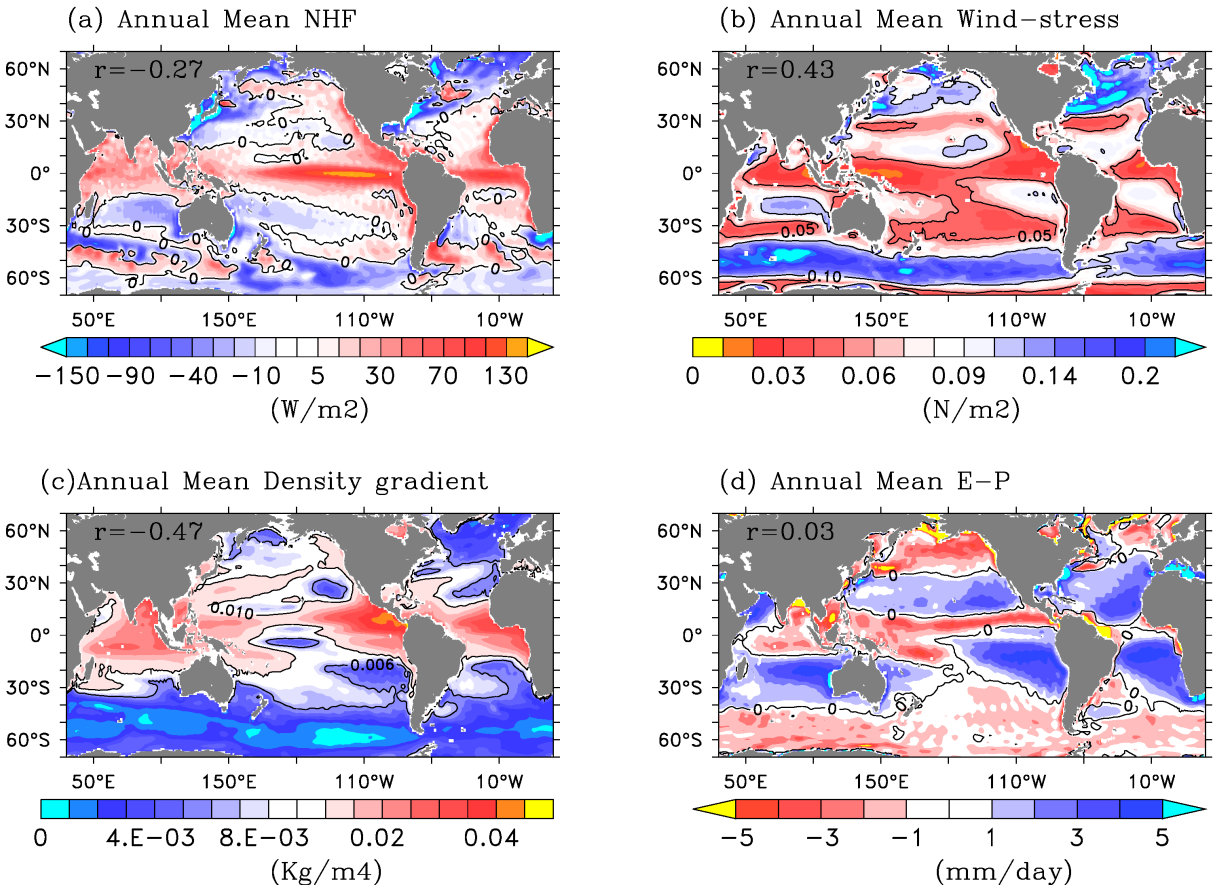

Fig 4: GECCO2 annual mean fields: (a) Net heat flux (NHF); positive/negative sign indicates the ocean is gaining/losing heat, (b) wind-stress, (c) density gradient (kg/m^4) between the surface and 100m depth, and (d) evaporation minus Precipitation (E-P). Colour code is in such a way that blue shading represents favourable for deep MLD and red shading for shallow mixed layers. Spatial correlation (r) between the forcing variable and the annual mean MLD (Fig 2a) is shown at the top left corner of the corresponding subplot.

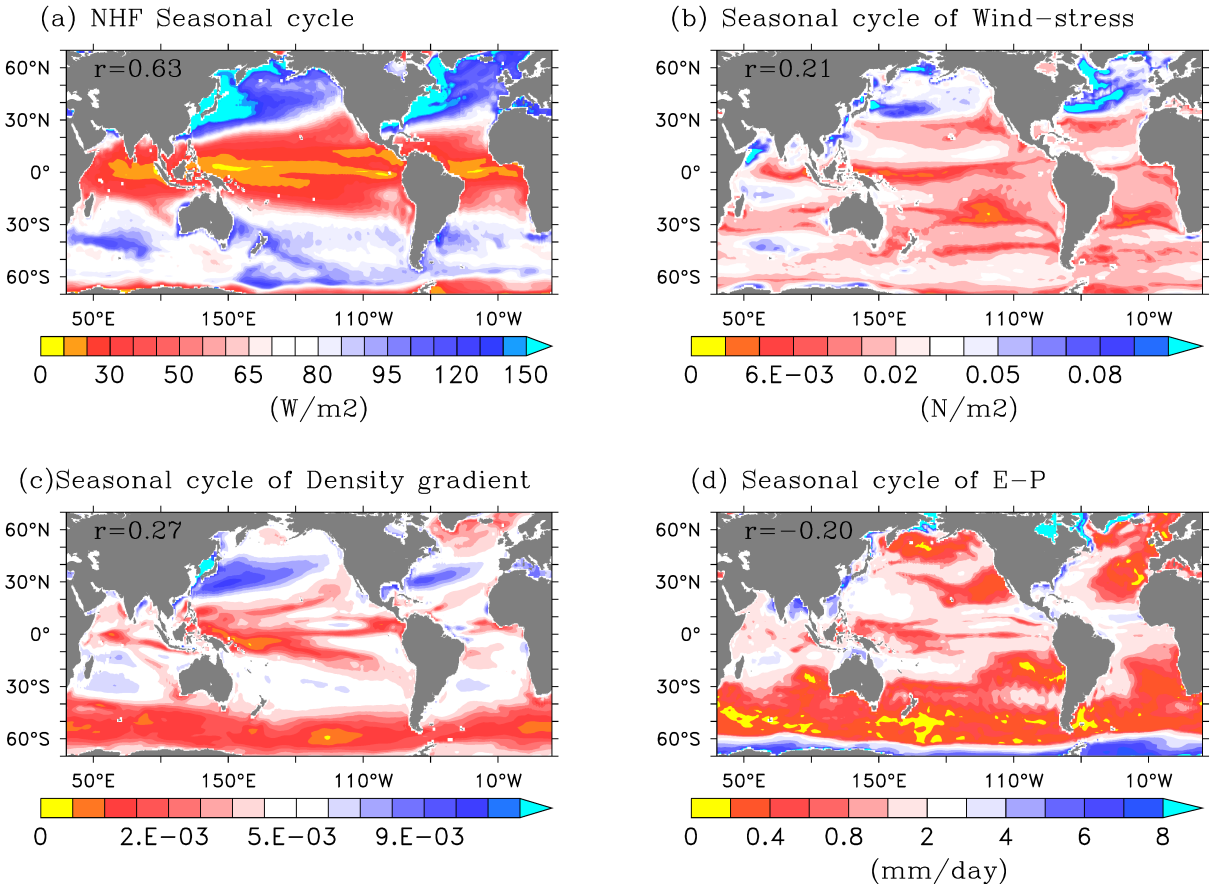

Fig 5: Seasonal amplitude of GECCO2 variables (computed as the standard deviation of the monthly climatology): (a) Net heat flux (NHF), (b) wind-stress, (c) density gradient (kg/m^4) between the surface and 100m depth, and (d) evaporation minus Precipitation (E-P). Spatial correlation (r) between the seasonal change of the forcing variable and the MLD (relative to the annual mean as in Fig 2b) is shown at the top left corner of the corresponding subplot.

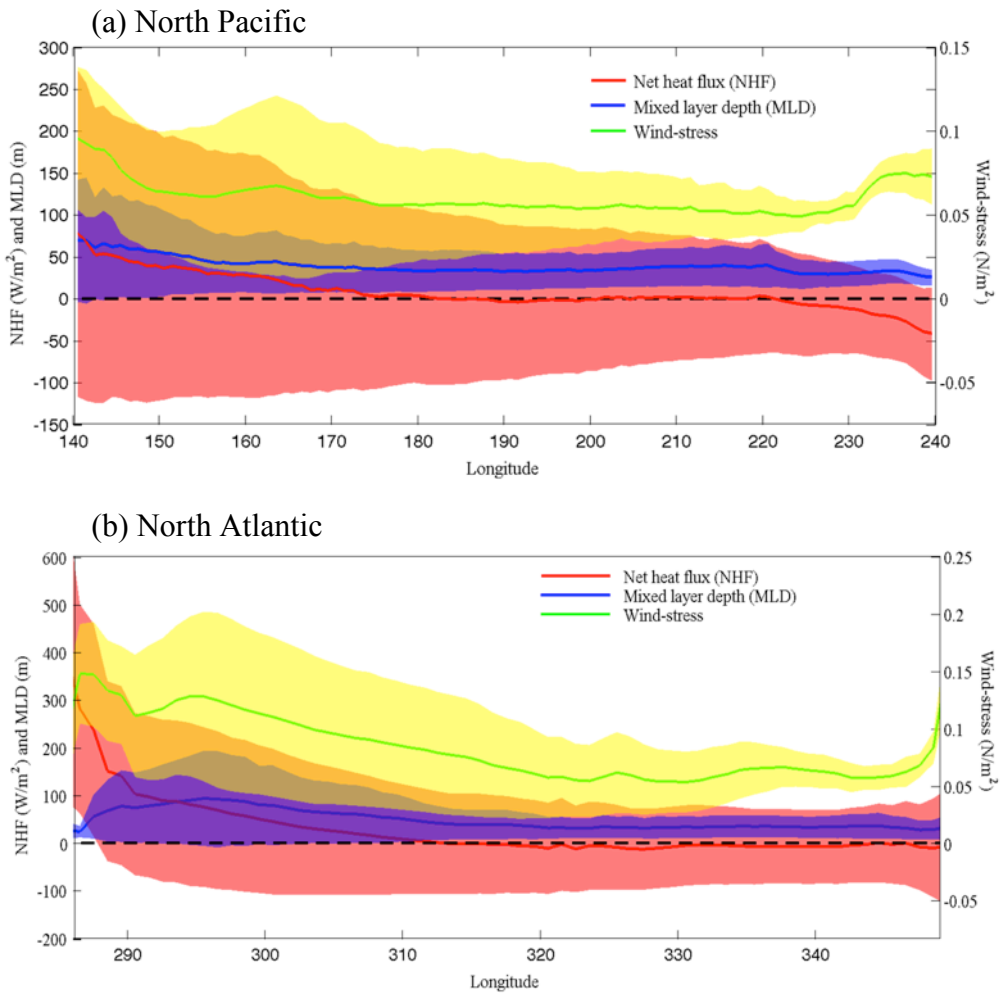

Fig 6: The annual mean MLD, net heat flux (NHF) and wind-stress (from GECCO2) averaged along (a) 30º-32ºN (North Pacific) and (b) 33º-35ºN (North Atlantic). The positive/negative heat flux (NHF) values indicate that the ocean is losing/gaining heat. The coloured shading represents the corresponding seasonal amplitude change at each grid point (light red for NHF, light blue for MLD and light yellow is for wind-stress).

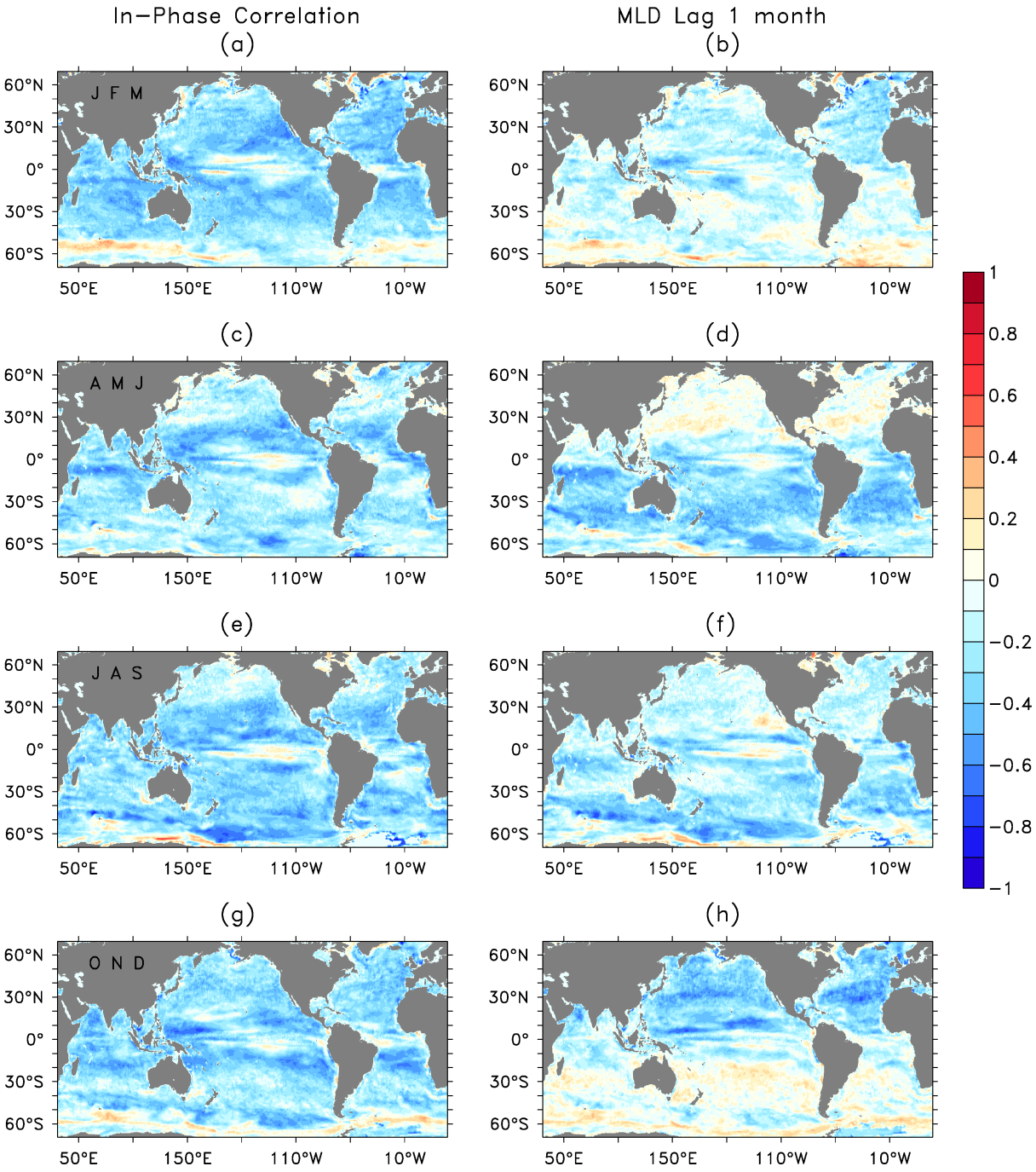

Fig 7: Cross correlation of net heat flux (NHF) and MLD anomalies in different seasons from GECCO2. Left column shows concurrent correlations and the right column represents the corresponding one-month lag correlations, where MLD lags the forcing by one month. The rows represent from top to bottom the different seasons: January-March (JFM), April-June (AMJ), July- September (JAS), and October-November (OND). Significant (95%) non-zero correlation value is ±0.1.

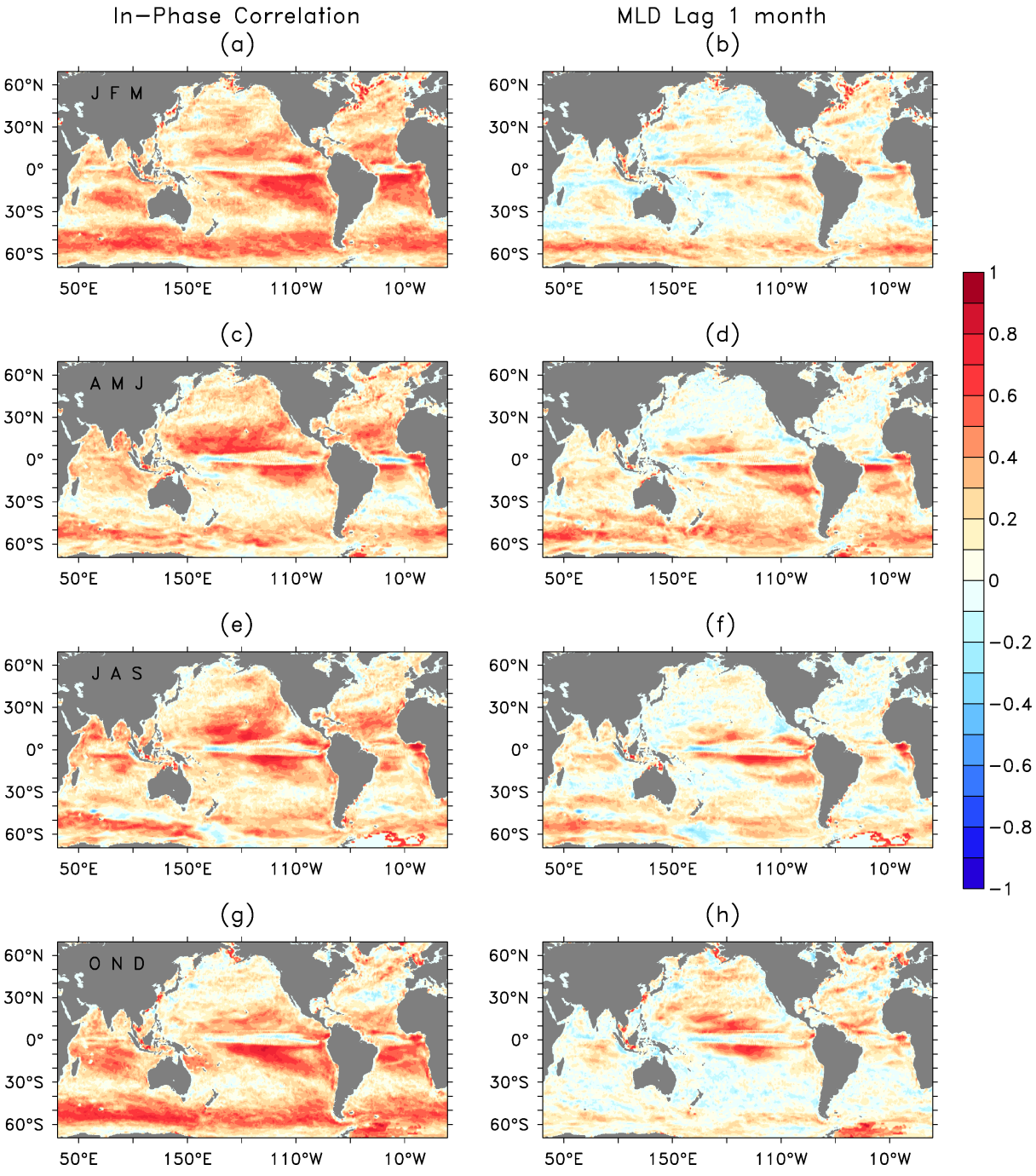

Fig 8: Cross correlation of wind stress (TAU) and MLD anomalies in different seasons from GECCO2. Left column shows concurrent correlations and the right column represents the corresponding one-month lag correlations, where MLD lags the forcing by one month. The rows represent from top to bottom the different seasons: January-March (JFM), April-June (AMJ), July- September (JAS), and October-November (OND). Significant (95%) non-zero correlation value is ±0.1.

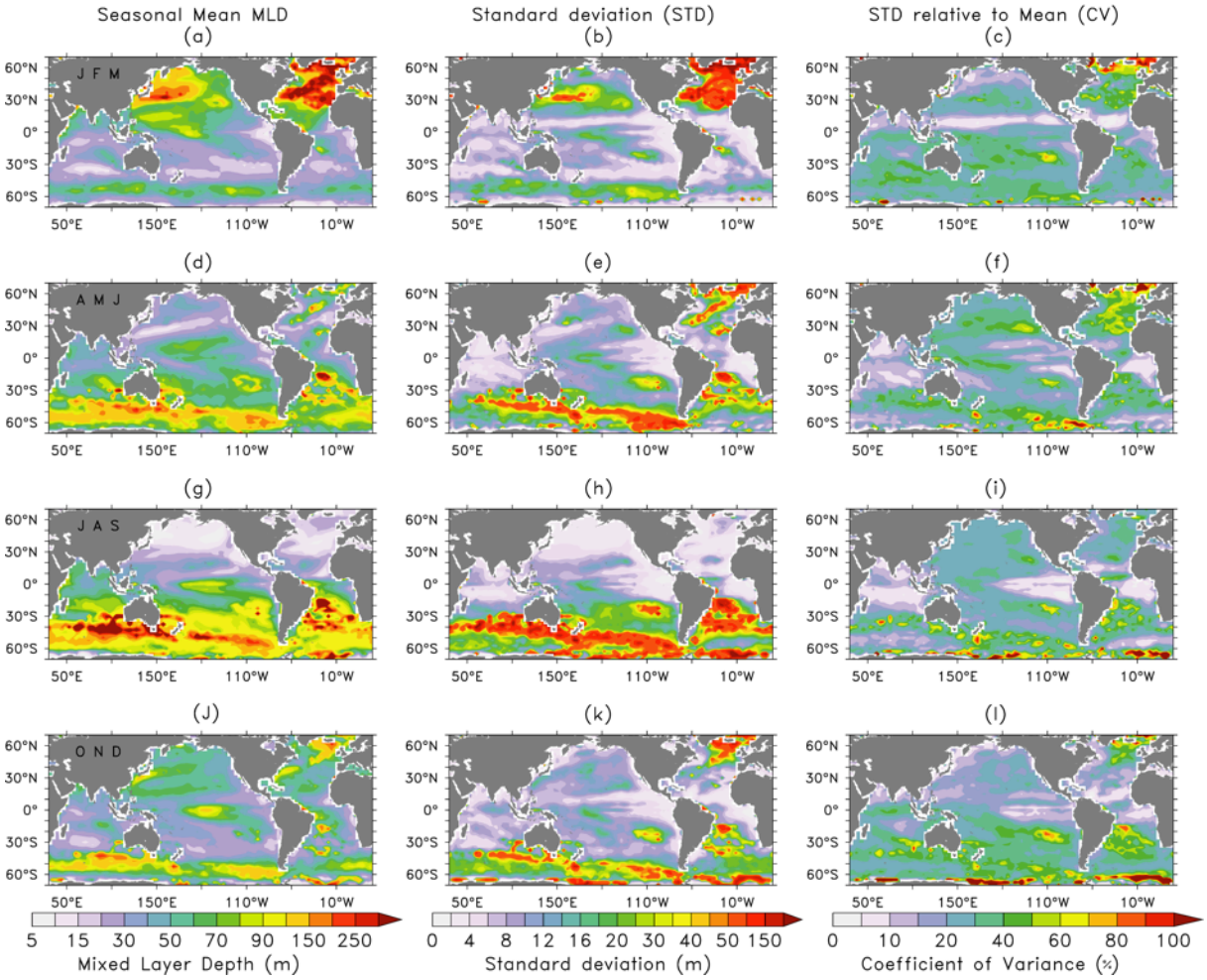

Fig 9: Seasonal statistics of MLD as in Fig 1 but for the ACCESS-KPP coupled model.

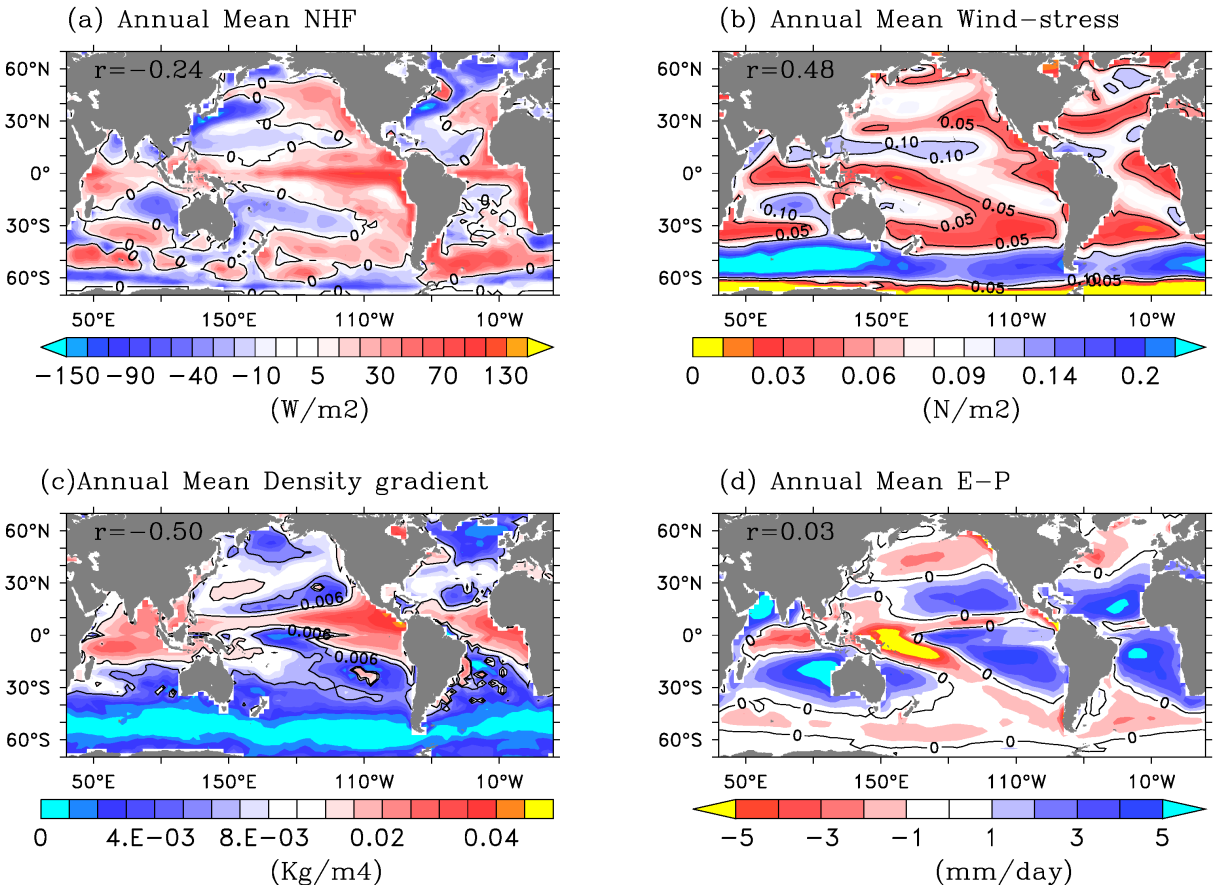

Fig 10: ACCESS-KPP annual mean fields (same as in Fig 4). Spatial correlation (r) between the forcing variable and the annual mean MLD (in Fig 12a) is shown at the top left corner of the corresponding subplot.

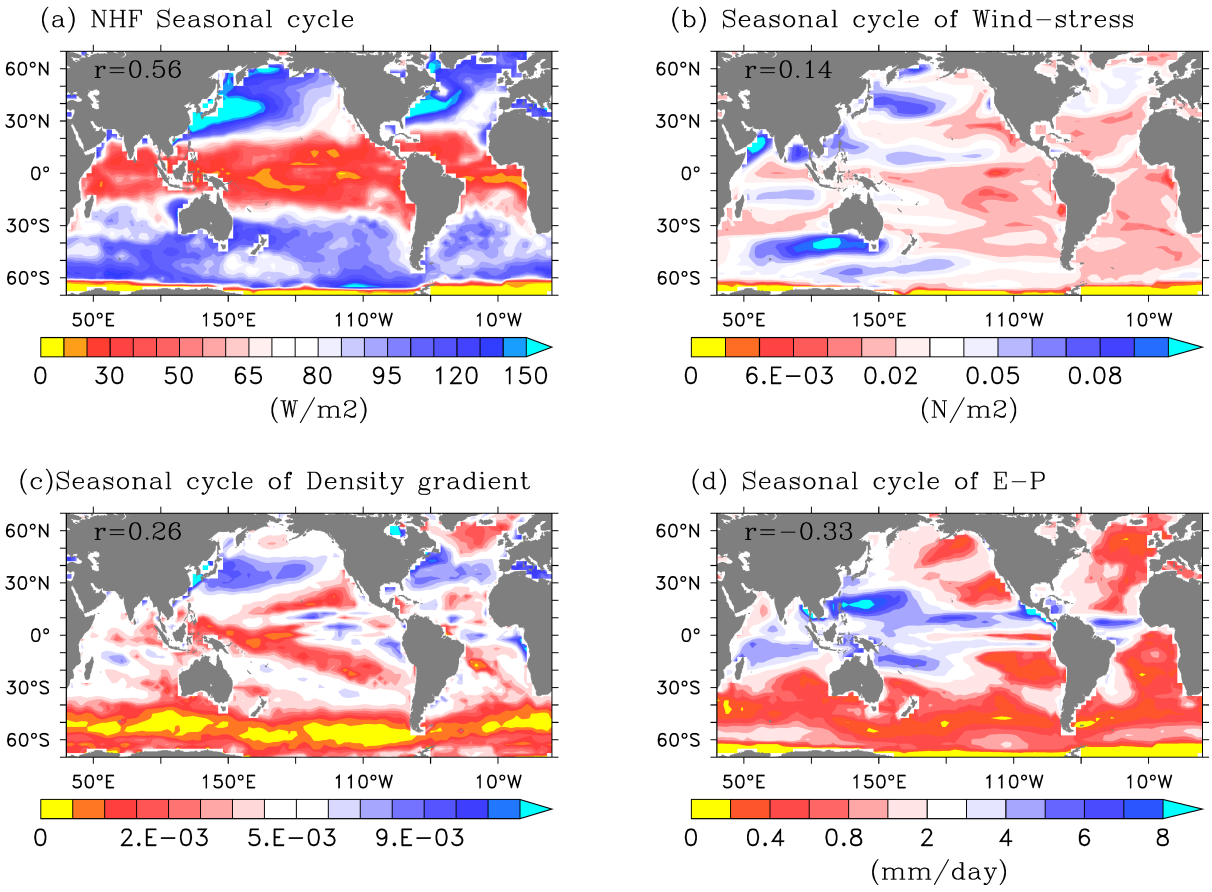

Fig 11: Seasonal amplitude of ACCESS-KPP forcing variables (same as in Fig 5). Spatial correlation (r) between the seasonal change of the forcing variable and the MLD (relative to the annual mean as in Fig 12b) is shown at the top left corner of the corresponding figure.

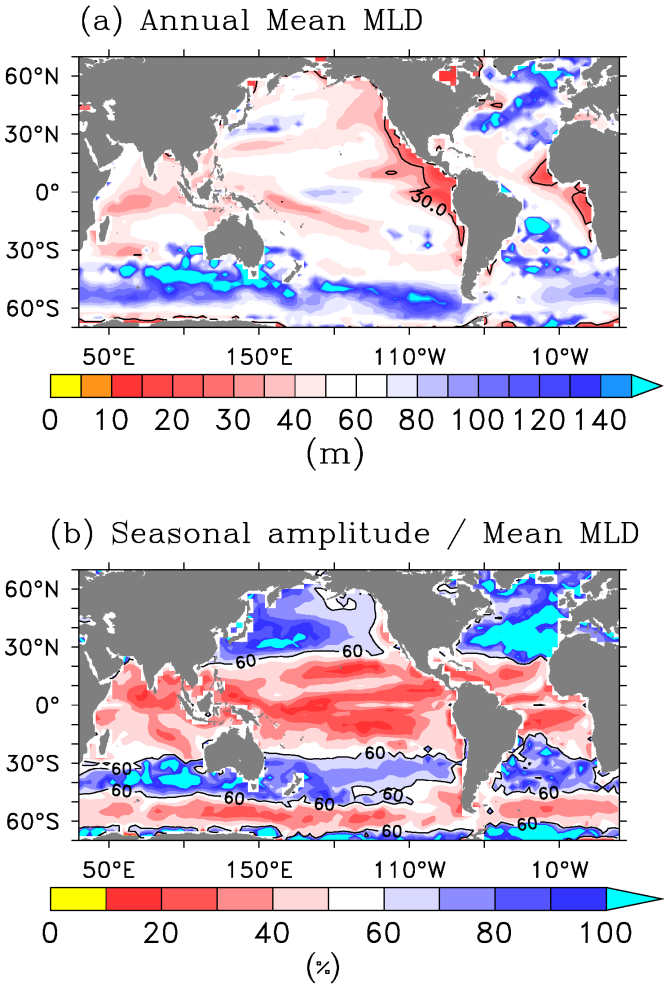

Fig 12: (a) Annual mean MLD estimated from ACCESS-KPP simulated density profiles (30m contour represents the shallow mixed layer), and (b) Seasonal amplitude of MLD relative to the annual mean MLD, with contour of 60% variability (similar to Fig 2).

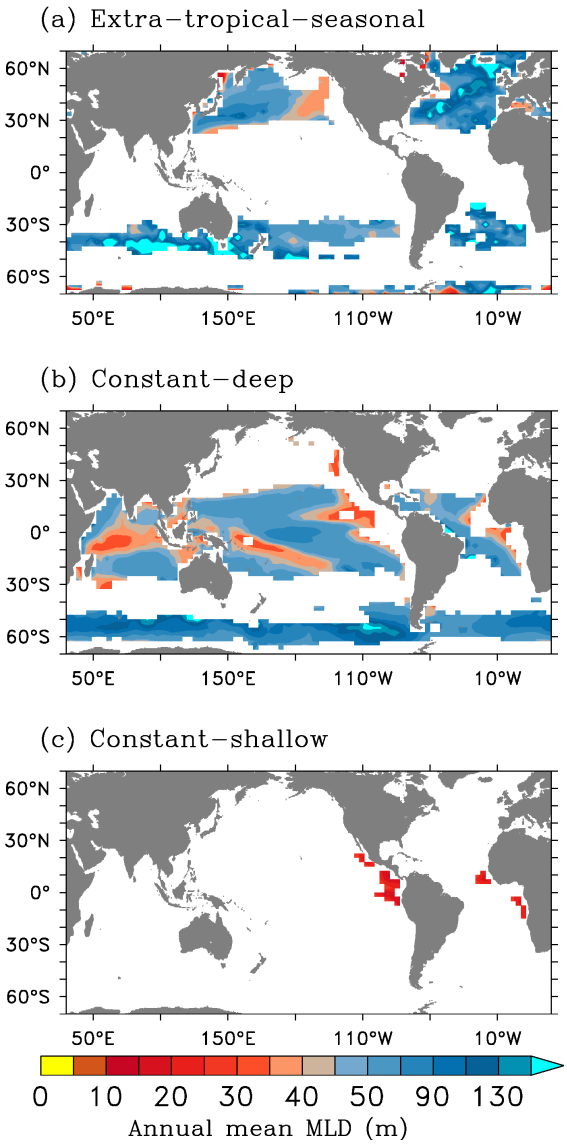

Fig 13: Different MLD regimes based on ACCESS-KPP simulation (same as in Fig 3)

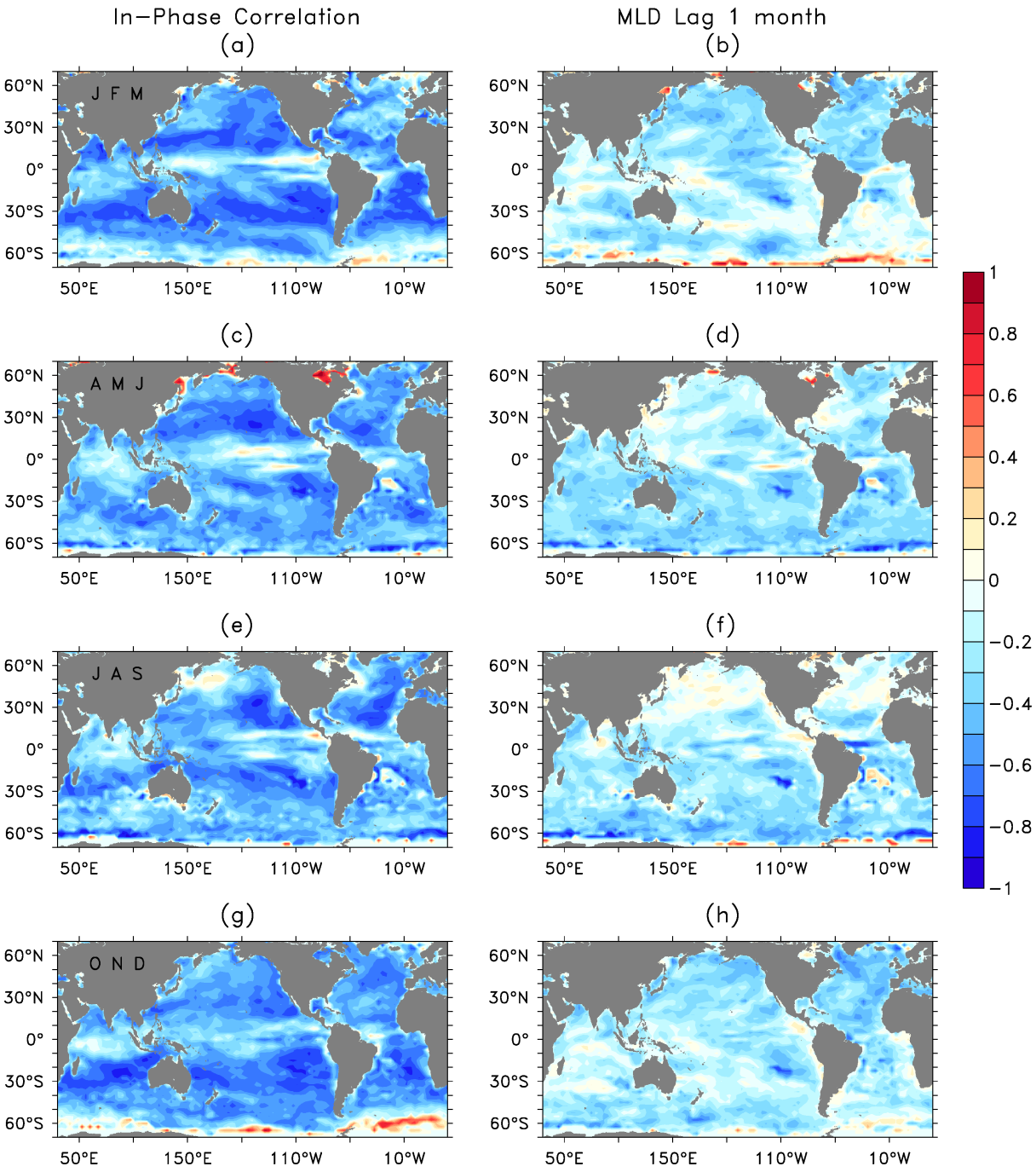

Fig 14: Cross correlation of net heat flux (NHF) and MLD anomalies in different seasons as in Fig 7 but for the ACCESS-KPP model. Significant (95%) non-zero correlation value is ±0.1.

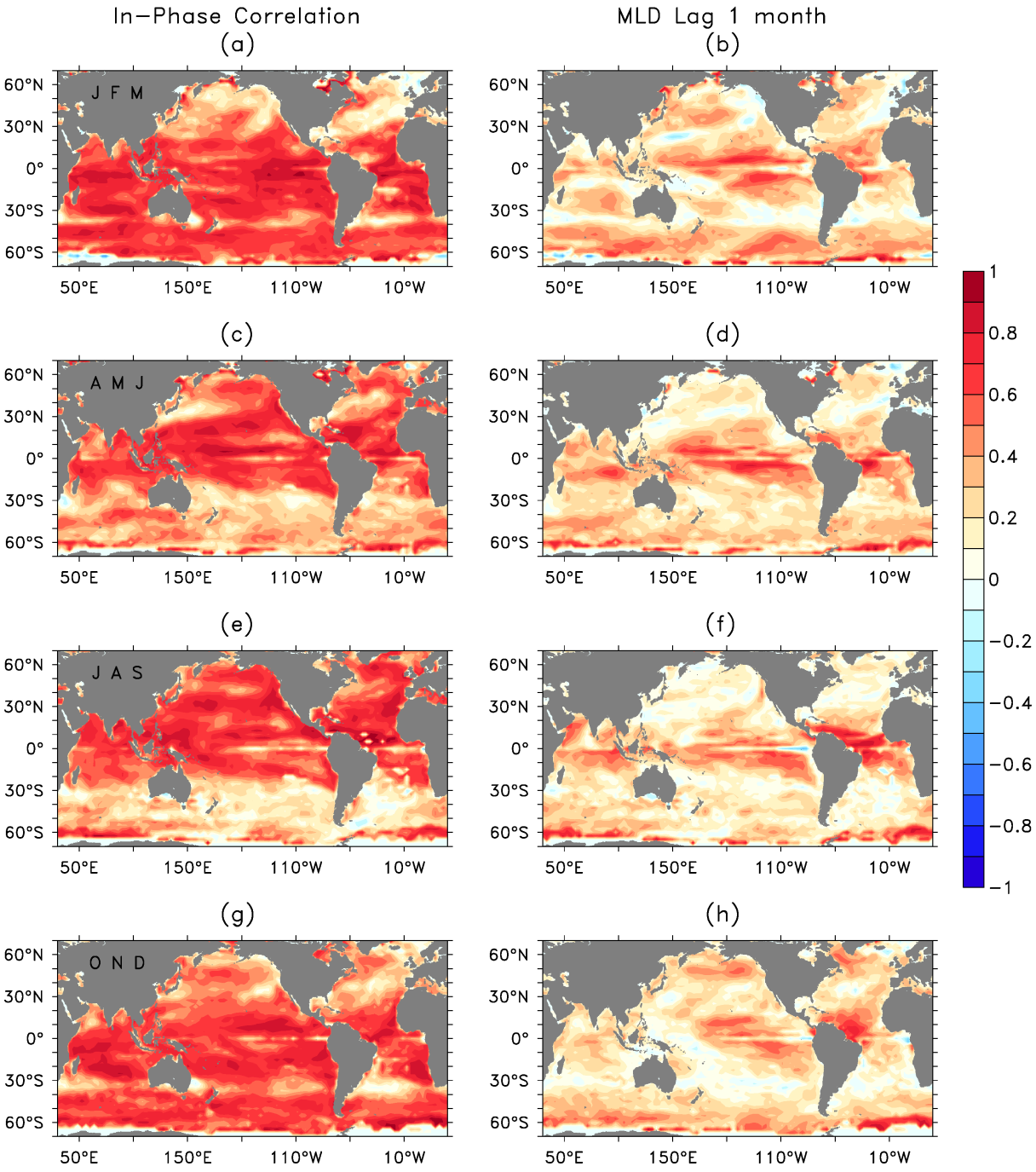

Fig 15: Cross correlation of wind-stress (TAU) and MLD anomalies in different seasons as in Fig 8 but for the ACCESS-KPP model. Significant (95%) non-zero correlation value is ±0.1.

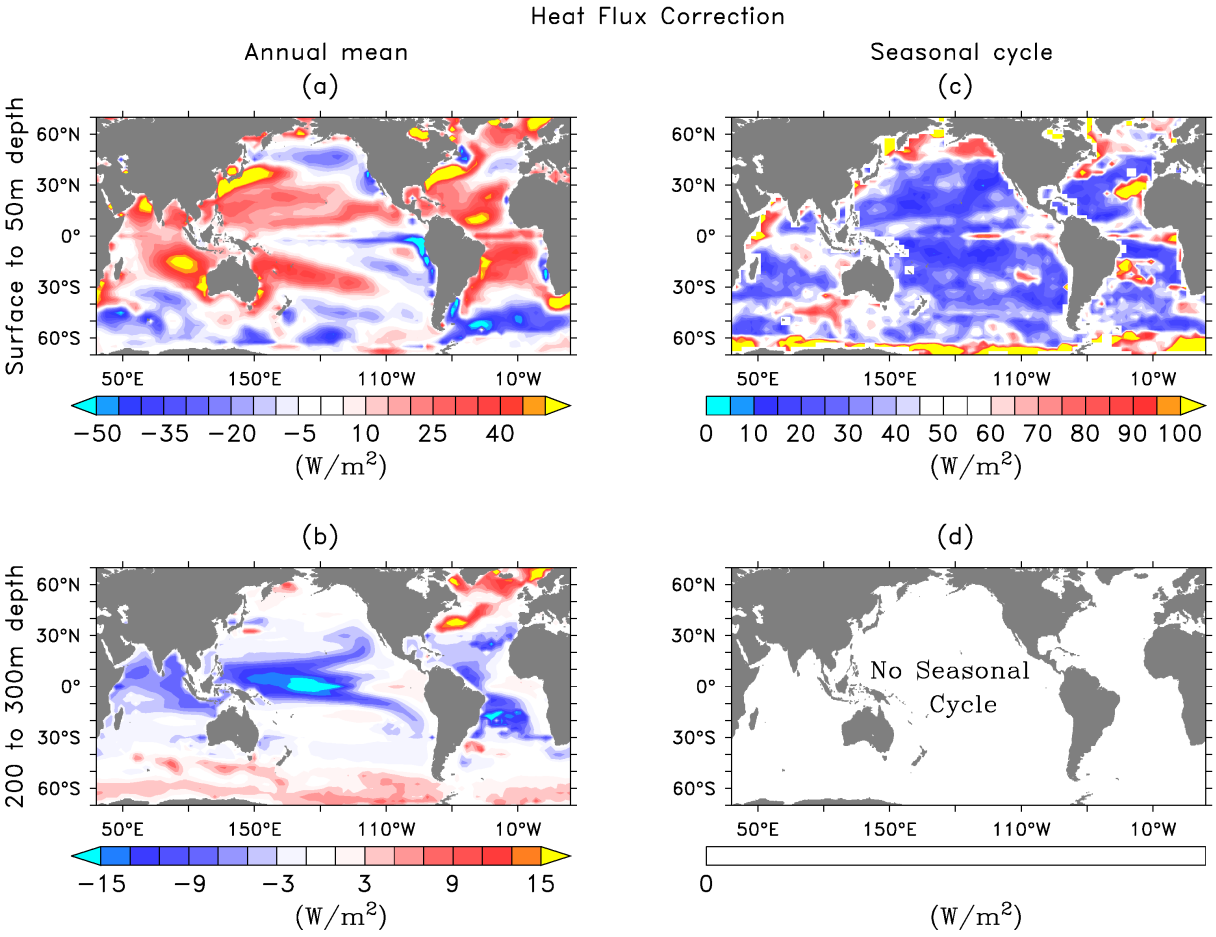

Fig 16: Annual mean (a, b) and seasonal cycle (c, d) of heat flux correction applied on the model levels (top) surface to 50m, and (bottom) 200-300m depth. The actual flux correction at each model level is in W/m^3 and here we multiplied with the thickness of all the layers (50m and 100m, respectively) to show the values in units of W/m^2. Seasonal cycle corresponds to the standard deviation of monthly flux correction in W/m^2. The deeper levels have no seasonal cycle corrections.

Supplementary figures

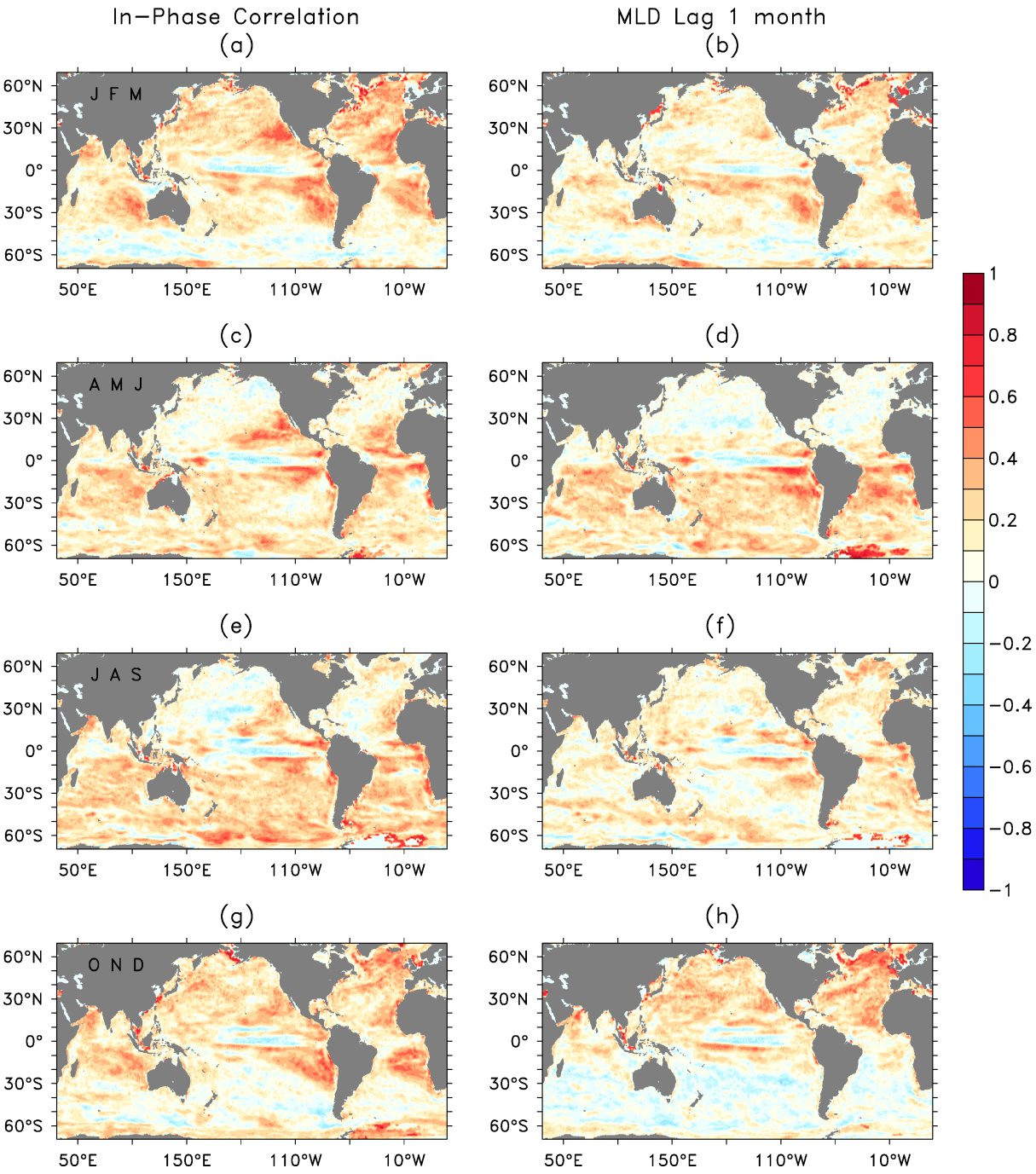

SFig 1: Cross correlation of E-P and MLD anomalies in different seasons from GECCO2. Left column shows concurrent correlations and the right column represents the corresponding one-month lag correlations, where MLD lags the forcing by one month. The rows represent from top to bottom the different seasons: January-March (JFM), April-June (AMJ), July-September (JAS), and October-November (OND). Significant (95%) non-zero correlation value is ±0.1.

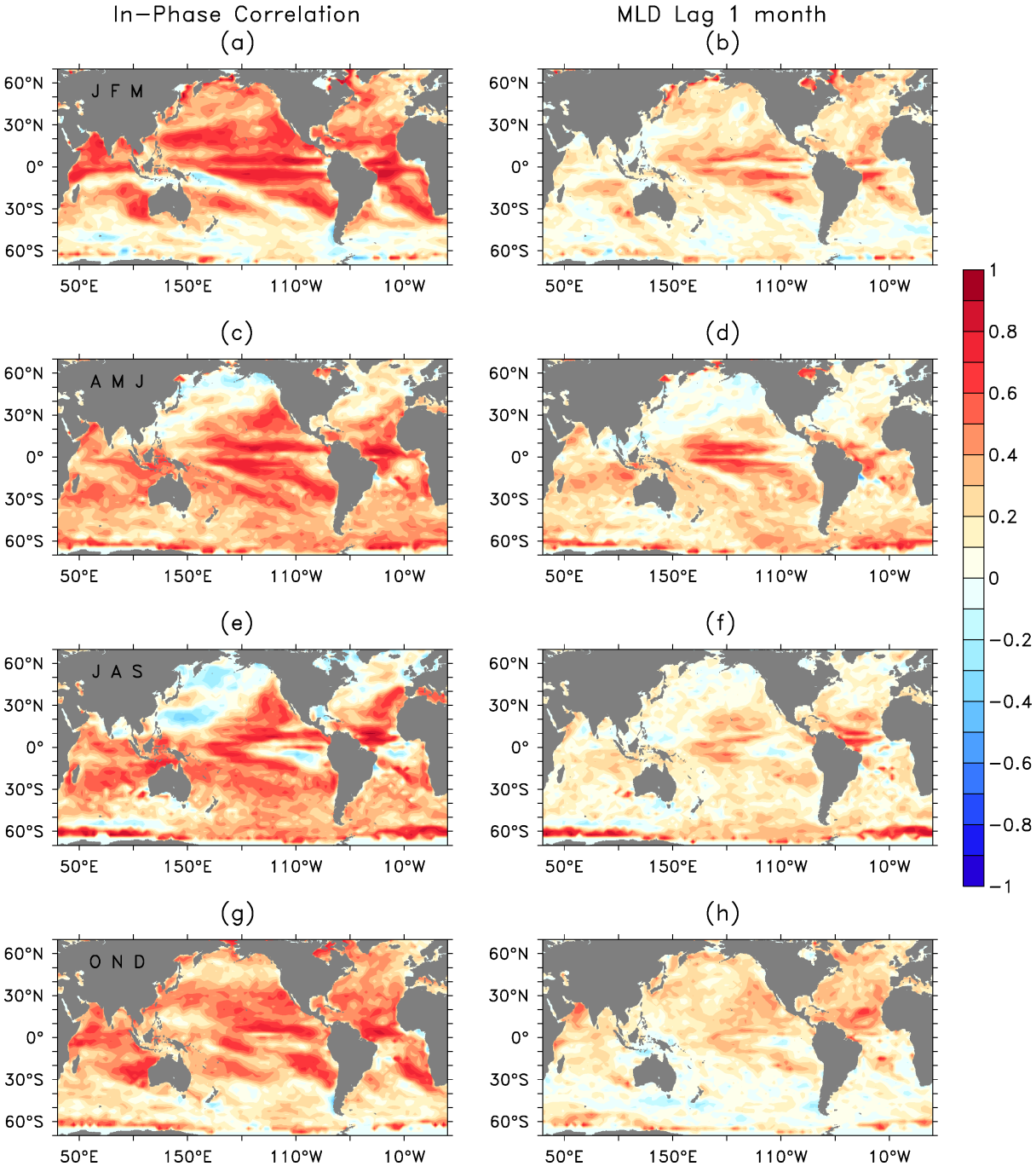

SFig 2: Cross correlation of E-P and MLD anomalies as in SFig 1 but for the ACCESS-KPP coupled model. Significant (95%) non-zero correlation value is ±0.1.

Table 1: Spatial correlation of variables in model and reanalyses data. The hyphen represents missing or no data.

ACCESS-KPP		GECCO2	NCEP-GODAS	SODA
MLD	Mean	0.61	0.44	0.62
	Seasonal Cycle	0.57	0.44	0.58
NHF	Mean	0.71	0.68	–
	Seasonal Cycle	0.86	0.84	–
TAU	Mean	0.72	0.83	0.84
	Seasonal Cycle	0.53	0.54	0.62
E-P	Mean	0.65	0.83	–
	Seasonal Cycle	0.31	0.79	–

Table 2: Spatial correlation of variables in GECCO2 and other reanalyses. (The values in brackets are the spatial correlation of GODAS and SODA data). The hyphen represents missing or no data.

GECCO2		NCEP-GODAS	SODA
MLD	Mean	0.50	0.71 (0.57)
	Seasonal Cycle	0.54	0.72 (0.62)
NHF	Mean	0.75	–
	Seasonal Cycle	0.94	–
TAU	Mean	0.82	0.83 (0.96)
	Seasonal Cycle	0.65	0.80 (0.82)
E-P	Mean	0.76	–
	Seasonal Cycle	0.39	–